Lethaia
AN INTERNATIONAL JOURNAL OF PALAEONTOLOGY AND STRATIGRAPHY

A revised calcareous nannofossil biozonation for the Lower Jurassic (Hettangian–Lower Pliensbachian) of NW Europe

MARIA PAULSEN, NICOLAS THIBAULT AND ÁNGELA FRAGUAS

LETHAIA

The Mochras core, UK, an historic reference site for the study of Early Jurassic calcareous nannofossils, has been reinvestigated here across the Hettangian to Lower Pliensbachian. Both relative and absolute abundances of 24 calcareous nannofossil species reveal patterns and occurrences that define not less than 37 defined biohorizons. However, due to the low abundance of many of those species towards the base and top of their stratigraphical range, we observe large inconsistencies in first and last occurrences of these species. Instead, we consider records of first consistent and last consistent occurrences (FCOs and LCOs), as well as base and top of acme events, as more reliable biohorizons. Accordingly, we assess the reliability of our biohorizons and show that, in addition to previously established zonal and sub-zonal biomarkers, nine non-zonal biohorizons prove to be robust. Based on that, an updated biozonations scheme with additional subzones for NJB has been proposed and tested against other localities. □
Coccoliths, Early Jurassic, Hettangian, Pliensbachian, Biostratigraphy, Mochras Borehole

Maria Paulsen [maria.paulsen@monash.edu], School of Earth, Atmosphere and Environment, 9 Rainforest Walk, Monash University, Clayton, Victoria, 3800, Australia and Department of Geosciences and Natural Resource Management, University of Copenhagen, Øster Voldgade 10, Copenhagen 1350, Denmark; Nicolas Thibault ✉ [nt@ign.ku.dk], Department of Geosciences and Natural Resource Management, University of Copenhagen, Øster Voldgade 10, Copenhagen 1350, Denmark; Ángela Fraguas [angela.fraguas@urjc.es], Departamento de Biología y Geología, Física y Química Inorgánica y Grupo de Investigación en Dinámica de la Tierra y Evolución del Paisaje (Dynamical), ESCET, Universidad Rey Juan Carlos, 28933 Móstoles, Spain; *manuscript received on 14/02/2023; manuscript accepted on 27/06/2023; manuscript published on 23/10/2023 in* Lethaia 56(3).

During the Early Jurassic, coccolithophores began to spread and evolve rapidly across the ocean and thereby experienced one of its most important radiation events (Mattioli & Erba, 1999; Bown *et al.* 2004; van de Schootbrugge *et al.* 2005; Erba, 2004; Wiggan *et al.* 2018; Peti & Thibault, 2022). Because of their burst in abundance and diversity, calcareous nannofossils have been considered a helpful biostratigraphical tool for dating Lower to Middle Jurassic rocks (Bown & Cooper 1998; Mattioli & Erba 1999; Veiga de Oliveira *et al.* 2007; Perilli *et al.* 2010; Mattioli *et al.* 2013; Fraguas *et al.* 2015, 2018; Peti *et al.* 2017; Ferreira *et al.* 2019; Cifer *et al.* 2022; Visentin *et al.* 2023). While the first erected biostratigraphical schemes for the Early Jurassic were relatively coarse (Bown 1987; Bown & Cooper 1998; Mattioli & Erba 1999), the recently revised scheme of Ferreira *et al.* (2019) offers numerous additional subzones for the Southern part of the peri-Tethys domain that opens the door for calcareous nannofossils as truly useful and precise tools for dating rocks of that age.

Revised taxonomy has also led to the re-evaluation of some taxa during the last three decades. Namely, the genera *Similiscutum* (de Kænel & Bergen 1993; Mailliot *et al.* 2023) for the Pliensbachian–Toarcian, *Biscutum* (Mattioli *et al.* 2004) for the same time interval, *Crepidolithus* (Fraguas & Erba 2010; Fraguas 2014) for the Upper Sinemurian–Pliensbachian, and *Lotharingius* (Mattioli 1996; Fraguas & Young 2011; Ferreira *et al.* 2017) for the Upper Pliensbachian–Lower Aalenian time interval. These contributions had important consequences for the revision of biostratigraphical schemes of the Western peri-Tethys domain, i.e., the Lusitanian Basin (Mattioli *et al.* 2013; Ferreira *et al.* 2019) and for the Cantabrian Range/N Spain (Fraguas *et al.* 2015, 2018). The biostratigraphical scheme of Bown & Cooper (1998) essentially relied on the original work of Bown (1987) on the Mochras core; hence, in the Northwest European domain (or Boreal part of the peri-Tethys), since then, this record had not been re-evaluated. A similar revision of the Boreal nannofossil biostratigraphical

https://doi.org/10.18261/let.56.3.4

scheme is, however, needed as Peti & Thibault (2022) have shown that several subzones of Ferreira *et al.* (2019) could be applied to the Sancerre-Couy core record. Moreover, in Early Jurassic sediments, issues of preservation come in addition to very low total nannofossil abundance, which potentially affects the reliability of bioevents based on relatively rare taxa. This reliability has not been assessed so far.

Besides using rare taxa as biomarkers, two other issues arise regarding the existing biozonation schemes. One issue that still remains for the earliest part of the Jurassic is the long range of existing biozones. The second issue is the consistency of first occurrence (FO) events as biozonal markers. As stated above, the reliability of Lower Jurassic FOs needs to be assessed thoroughly because the combination of moderate to poor preservation and very low total nannofossil abundance is responsible for inconsistent recorded occurrences in single locations that likely imply large uncertainties in their large-scale correlation. Moreover, a number of Early Jurassic evolutionary events have been suggested to be time-transgressive between the Boreal and Southern part of the peri-Tethys domain (Perilli *et al.* 2010; Fraguas *et al.* 2015, 2018; Peti *et al.* 2017). Significant improvements have been made in the Palaeogene, Cretaceous and Mesozoic nannofossil biostratigraphical schemes using base and top acme events, as well as first and last consistent occurrences (FCOs and LCOs, respectively) that rely on absolute abundance patterns rather than in the presence/absence and/or semi-quantitative data (Thibault *et al.* 2012a; Agnini *et al.* 2014; Ferreira *et al.* 2019). Inspired by these improvements, we document here such patterns and assess the reliability of our biohorizons in the Hettangian to Lower Pliensbachian of the reference Mochras borehole.

Study location

During the Early Jurassic, the supercontinent Pangaea broke up, leading to the formation of an epicontinental seaway in NW Europe as part of the Western Tethys Ocean (Bassoullet & Baudin 1994; Hermoso *et al.* 2009). During that time the investigated site, the Mochras Farm (Llanbedr) borehole, was located between palaeolatitudes of 30–45° N (Coward *et al.* 2003; Korte *et al.* 2015). Most of this region was traversed by epicontinental seas forming the Laurasian Seaway (Fig. 1A, B), which connected the peri-Tethys domain in the S to the Boreal Sea via the Viking Corridor in the N (Korte *et al.* 2015). Lower Jurassic strata of the Mochras borehole consist of interbedded mud- and siltstone (Fig. 1C), characterizing a hemipelagic environment (Tappin *et al.* 1994). The momentum of the Early Jurassic Earth System and Timescale (JET) NERC and ICDP research project (Hesselbo *et al.* 2013) offered the occasion to re-examine this important interval.

Methods

Calcareous nannofossils

A total of 102 samples spanning the Hettangian to Lower Pliensbachian of the Mochras core were investigated for calcareous nannofossils. All samples were carefully disaggregated and 150 mg (±0.5 mg) of dry sediment dispersed into 50 mL of Silex water. The suspension was homogenized with a magnetic stirrer and treated in a sonic bath for about 8–10 sec, if necessary. Microscopic coverslips were weight before and, after deposition of 0.75 mL of that suspension evenly spread on the surface of the coverslips. After drying slowly, the microscopic coverslip was mounted onto a microscopic slide with a Norland optical adhesive. Several studies have described a similar method (e.g. Koch & Young 2007; Thibault *et al.* 2012a,b; Peti *et al.* 2017) and have proven a high reproducibility with a minimal error margin for counting absolute calcareous nannofossil abundances. As the exact weight of dry sediment deposited on the known area of the coverslip can be calculated, absolute abundances can be reported in number of specimens per gram of sediment (Peti *et al.* 2017).

Semi-quantitative counts of coccolith species were performed with a Leica 750P light microscope at a magnification of 1000x. For this study only observed coccolith species have been counted. Therefore, the threshold of 200 specimens per sample is considered as significantly high due to the limited number of species (max. 17 species in the Lower Pliensbachian and much fewer in the Hettangian to Sinemurian, see (Reggiani *et al.* 2010)). Furthermore, statistical work shows that by counting 200 specimens per sample the probability of not recording very rare taxa (representing less than 1% of the total assemblage) is lower than 15% (Hay 1972; Reggiani *et al.* 2010). Due to the low abundance of specimens in that part of the Jurassic, decisions were taken regarding the total number of specimens counted per slide for time optimisation. Varying amounts of specimens, between 200 and 300, were counted for the Upper Sinemurian and Pliensbachian while only approximately 100–150 specimens, across at least 300 fields of view (FOVs) were counted for the Hettangian to Lower Sinemurian, an interval where the total nannofossil abundance is particularly low.

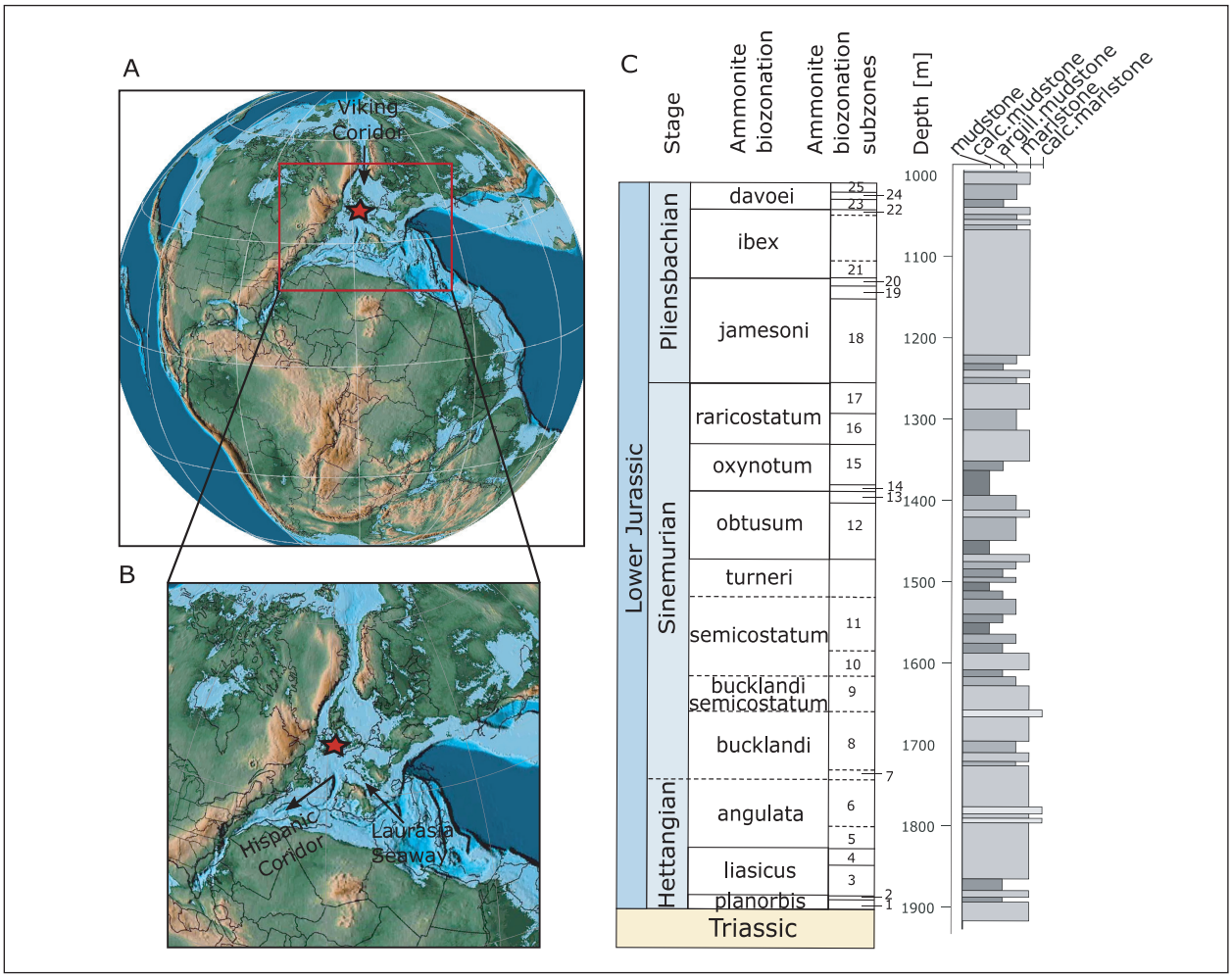

Fig. 1. A, B, palaeogeographical position of the Mochras borehole indicated with a red star; A, Early Jurassic global palaeogeography. B, detail of the area within the red square in (A) (modified from Scotese *et al.* 2016). C, complete stratigraphical succession of the studied interval, together with ammonite zones and ammonite subzones (modified after Copestake & Johnson 2013). Simplified lithological log of the Mochras core derived from Ullmann *et al.* (2022). Key for ammonite subzones: 1) *planorbis*, 2) *johnstoni*, 3) *portlocki*, 4) *laqueus*, 5) *extranodosa*, 6) *complanata–depressa*?, 7) *conybeari*, 8) *rotiforme*, 9) *bucklandi–lyra*, 10) *scipionianum*, 11) *sauzeanum*, 12) *obtusum–stellare*, 13) *denotatus*, 14) *simpsoni*, 15) *oxynotum*, 16) *densinodulum– raricostatum*, 17) *macdonnelli–aplanatum*, 18) *taylori–polymorphus*, 19) *brevispina*, 20) *jamesoni*, 21) *masseanum*?*–valdani*, 22) *luridum*, 23) *maculatum*, 24) *capricornus*, 25) *figulinum* (from Storm *et al.* 2020).

Coccolith sizes were obtained by measurements in ImageJ, and the error of X+0.75 microns is estimated after 10 repetitive measurements of 10 coccoliths (following Suchéras-Marx *et al.* 2010).

By applying the etching and overgrowth criteria of Roth (1983), preservation of the calcareous nannofossil assemblages was evaluated. Thereby, a good (G) preservation was considered, if etching and overgrowth were not beyond stage 1, moderate (M) if either of the stages reaches stage 2 and poor (P) if either etching or overgrowth was reaching stage 3. Similar to Peti *et al.* (2017), samples are very poor (VP) if either etching or overgrowth was considered as stage 3 and species richness ≤3, and nearly barren (NB) if samples showed very few coccoliths and an etching and overgrowth at stage 4 *sensu* Roth (1983). Samples with no recorded coccoliths were considered as barren (B).

Determination of coccolith abundance and level of confidence of biohorizons

Counts of coccolith specimens were used to calculate the absolute abundance of each species (Eq. 1; N/g $\times 10^6$). As the size of one field of view (FOV= $\pi \times$ (0.09 mm)^2), the total area of the slide (768 mm^2) and

the amount of dry sediment on a slide are known, the absolute abundance per gram of sediment was calculated (Eq. 1).

Eq. 1: Absolute abundance of coccoliths per g of sediment (coccoliths/g sediment $\times 10^6$)
= [coccoliths/FOV $\times$ cover-slip area/area of one FOV)/mass of sediment on slide (g)] $\times 10^6$

Besides FOs and LOs, we chose to define the FCOs and LCOs, which are characterized at the base and top of stratigraphical intervals, where species are consistently recorded in more than two adjacent samples. Acme events are identified when statistic significant differences in abundance can be delineated. The statistically significance has been tested by applying an F-Test (Two-sample for Variances) before carrying out a Two-sample Unequal variance t-Test, with samples showing an abrupt consistent increase in absolute abundances (Appendix B).

Accordingly, we report the relative and absolute ages of our biohorizons using the orbitally calibrated age scale of Storm *et al*. (2020) whose 0 level was chosen at the base Sinemurian at a depth of 1741.4 m, and absolute age is 199.1 Ma following the latter authors. The calculated ages correspond to the average between top and bottom depths of biohorizons, while half of the difference between top and bottom depth allows the age uncertainty. Sample spacing for the studied interval is approximately 9.5 m, resulting in an average age spacing between samples of 0.139 Myr.

In order to evaluate the reliability of the recorded bioevents, we applied the categories of confidence proposed by Peti *et al*. (2017) as follows. Confidence is considered as low, if after the FO or preceding the LO, the species is recorded discontinuously over a large stratigraphical interval with sporadic occurrences. Confidence level is considered medium, if a limited number of sporadic occurrences is recorded over a short, restricted interval, immediately following the FO or preceding the LO. A high level of confidence is considered when the species is showing a robust consistent record after the FO or preceding the LO. Thereby, FCOs and LCOs, as well as base and top of acme events, are considered to represent robust bioevents as they mark the onset and end of a consistent record, respectively. In addition to absolute abundances, we also used categories of semi-quantitative abundances in order to allow comparison to previous studies that commonly used these categories. Semi-quantitative counts are similar to the categories of Peti *et al*. (2017) and defined as follows. A: abundant (≥10 spp./FOV), C: common (=1-10 spp./FOV), F: frequent (=1spp./10 FOVs), R: rare (=1spp./10-100 FOVs), VR: very rare (=1 spp./101-299 FOVs) and S: single (=1spp./300FOVs).

Results

Taxonomic remarks

The taxonomic concepts follow Bown (1987) and Bown & Cooper (1998) for murolith coccoliths, and de Kænel & Bergen (1993) and Mattioli *et al*. (2004) for *Mazaganella* and *Similiscutum*, which are placolith coccoliths. Calcareous nannofossil species recognized in this study are illustrated in Figure 2 and listed in Appendix A.

Specimens of *C. crassus* have been subdivided after their size in *C. crassus* (averages of 8.5 ± 0.75 µm in size) and small *C. crassus* (average of 6.5 ± 0.75 µm in size), following Suchéras-Marx *et al*. (2010). Based on visual estimation of their wall thickness, specimens of *T. patulus* have been subdivided into *T. patulus* thin (approximately smaller than 4 µm in length after Chaumeil Rodríguez *et al*. 2022) and *T. patulus* thick (approximalty 5–7 µm in length after Chaumeil Rodríguez *et al.* 2022). The same concept has been applied on specimens of *C. granulatus* (*C. granulatus* thin, *C. granulatus* thick), following the suggestions of Chaumeil Rodríguez *et al*. (2022) and previous observations of Peti *et al*. (2017) and Mattioli *et al*. (2013).

Due to preservation issues, it was not always possible to differentiate between the subspecies of *P. liasicus* (*P. liasicus distinctus* and *P. liasicus liasicus*), or between the two distinct species of *Similiscutum* (*S. cruciulus* and *S. avitum*), hence explaining our use of the 'sensu lato' suffix. Additionally, those specimens for which species identification was not possible have been named after their genus (*Crepidolithus* sp., *Parhabdolithus* sp., *Crucirhabdus* sp. and *Mitrolithus* sp.). In a number of samples, some specimens could not be identified at genus and species level and have been therefore classified as 'non-identified coccoliths'.

Calcareous nannofossil abundances, stratigraphical ranges and confidence levels

The stratigraphical range of coccolith species is defined by their FO and/or LO. Both semi-quantitative and absolute abundances, as well as preservation of the analysed calcareous nannofossil assemblages, vary through the investigated record but remain relatively low. The state of preservation is poor on average, with only minor changes (see Supplementary Information B). Overall, these three parameters show

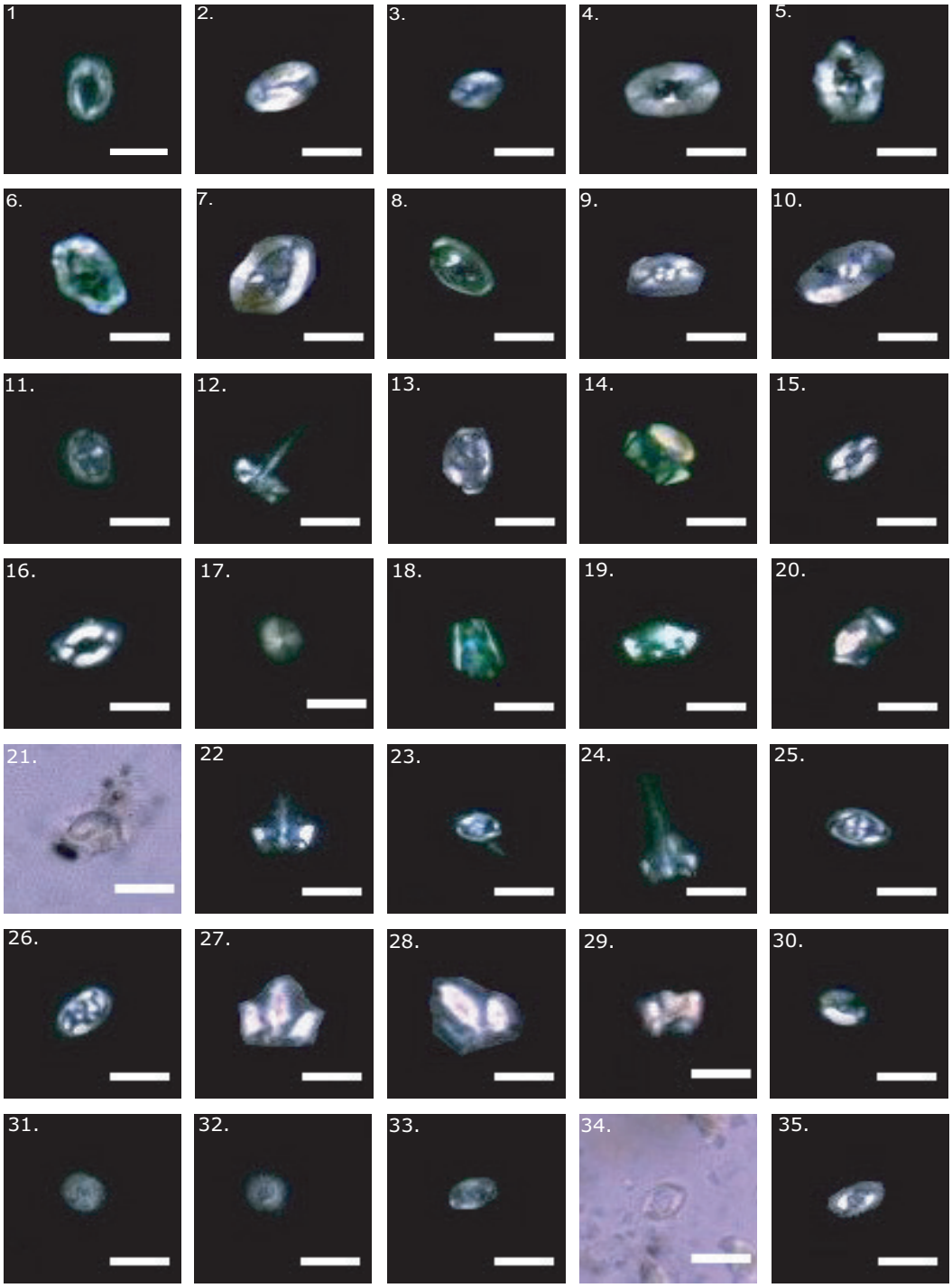

Fig. 2. Coccolith specimens encountered in this study. Unless otherwise stated, pictures are taken with polarized light. 1: *C.* cf. *C. cantabriensis* (ibex AZ, 1057.02), 2: *C. crassus* (ibex AZ, 1048.05 m), 3: small *C. crassus* (ibex AZ, 1057.02 m), 4: *C. crucifer* (ibex AZ, 1057.02 m), 5: *C. crucifer* (davoei AZ, 1017.09 m), 6: *C. granulatus* thick-walled (ibex AZ, 1039.72 m), 7: *C. granulatus* thick-walled (davoei AZ, 1017.09 m), 8: *C. granulatus* thin-walled (davoei AZ, 1017.09 m), 9: *C. pliensbachensis* (jamesoni AZ, 1156.33 m), 10: *C. pliensbachensis* (jamesoni AZ, 1156.33 m), 11: *C. primulus* (jamesoni AZ, 1156.33 m), 12: *C. primulus* (ibex AZ, 1116.05 m), 13: *M. protensa* (jamesoni AZ, 1248.51 m), 14: *M. elegans* (ibex AZ, 1094.56 m), 15: *M. elegans* (jamesoni AZ, 1202.00 m), 16: *M. elegans* (davoei AZ, 1017.09 m), 17: *M. elegans* spine (ibex AZ, 1097.74 m), 18: *M. jansae* (jamesoni AZ, 1116.05 m), 19: *M. lenticularis* (raricostatum AZ, 1303.73 m), 20: *M. lenticularis* (jamesoni AZ, 1202.00 m), 21: same as 20, natural light, 22: *P. liasicus distinctus* (jamesoni AZ, 1202.00 m), 23: *P. liasicus liasicus* (ibex AZ, 1057.02 m), 24: *P. liasicus liasicus* (ibex AZ, 1057.02 m), 25: *P. liasicus* s.l. (ibex AZ, 1106.27 m), 26: *P. liasicus* s.l. (ibex AZ, 1106.27 m), 27: *P. marthae* (semicostatum AZ, 1611.88 m), 28: *P. marthae* (semicostatum AZ, 1611.88 m), 29: *P. robustus* (ibex AZ, 1048.05 m), 30: *S. avitum* (ibex, AZ), 31: *S. cruciulus* (ibex AZ, 1106.27 m), 32: *Similiscutum* s.l. (ibex AZ, 1106.27 m), 33: *T. patulus* (thin, davoei AZ, 1017.09 m), 34: same as 33, natural light, 35: *T. patulus* (thick, jamesoni AZ, 1156.33 m), All scale bars represent 5µm.

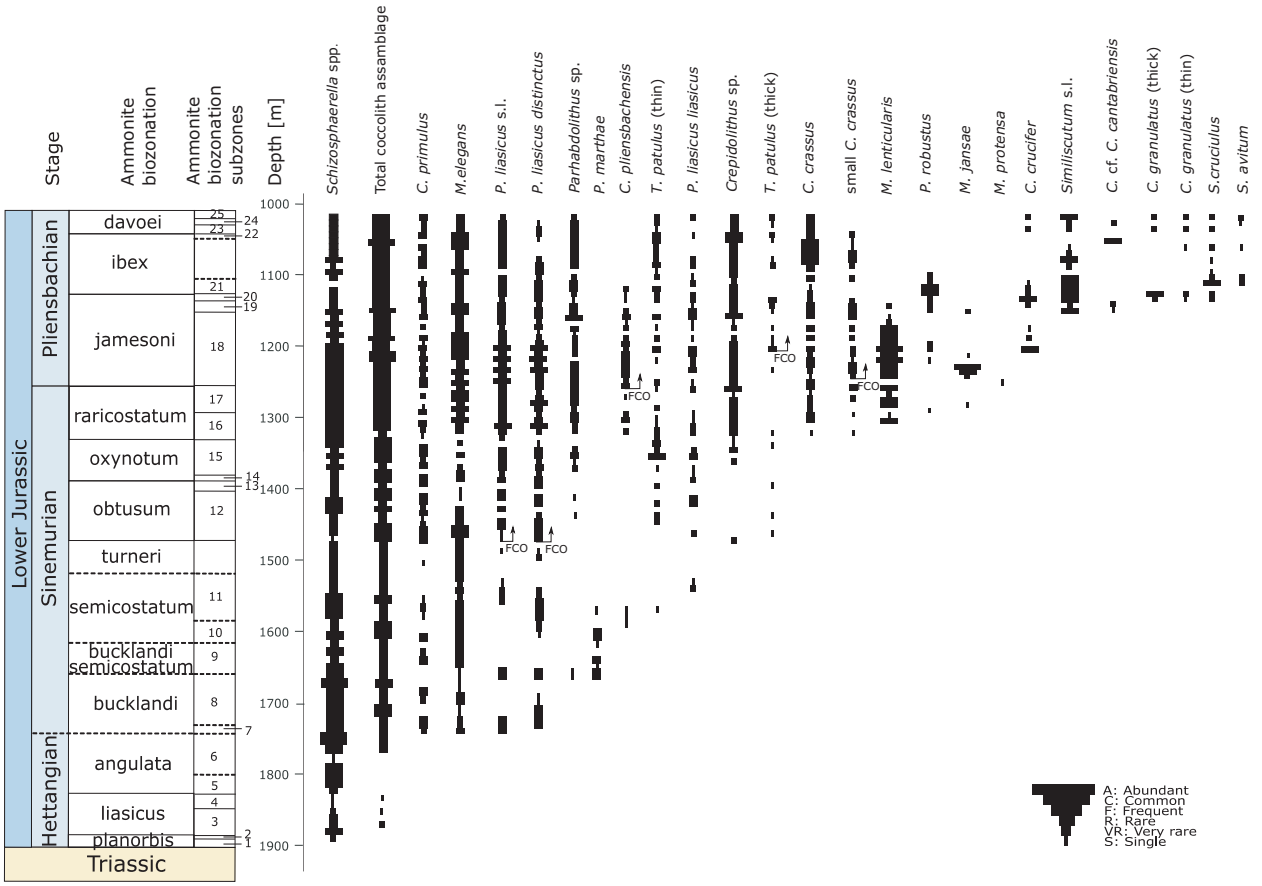

Fig. 3. Compiled ranges and semi-quantitative occurrences of calcareous nannofossils across the Hettangian-Lower Pliensbachian of the Mochras core, illustrating their diversification. A: abundant (≥10 spp./FOV), C: common (=1-10 spp./FOV), F: frequent (=1spp./10 FOVs), R: rare (=1spp./10-100 FOVs), VR: very rare (=1 spp./101-299 FOVs), S: single (=1spp./300FOVs). FCO represent the first consistent occurrence of a species.

an improving trend from the bottom to the top of the Mochras core (Fig. 3). The total coccolith assemblage varies between absent and common (C) (Fig. 3). In the following paragraphs, only coccolith species with significant variations throughout the core will be mentioned.

Crucirhabdus primulus shows a discontinuous record, being noted as absent in numerous samples above its FO, but overall varies between very rare (VR) and rare (R) for most of the studied interval. Changes in abundance for *M. elegans* appear more continuous. From its FO at 1739.19 m (bucklandi AZ) to the Lower raricostatum AZ (1318.26 m), *M. elegans* is mostly rarely observed, whilst for the upper part of the core (1318.26 m – 1017.09 m), it changes between R and frequent (F). Both *P. liasicus* s.l. and *P. liasicus distinctus* show discontinuous records due to their absence in numerous samples above their FOs in the lower part of the core, until the oxynotum/raricostatum AZs boundary (FCO – 1330.05 m), from where on, a more continuous trend is observed with variations between R and F, more often in the raricostatum to Early jamesoni AZs interval (1330.05 m – 1202.00 m). *Parhabdolithus marthae* was only rarely observed within a relatively short interval (1676.10 m – 1581.73 m). Occurrences of *C. pliensbachensis* are systematically characterized by a single specimen in samples of the Lower semicostatum AZ (1593.09 m – 1581.73 m). Subsequently, a long interval of absence of this species is recorded (1569.52 m – 1330.05 m). Thereafter, specimens of *C. pliensbachensis* were observed more often, although changing between absent, single (S), VR and R (1330.05 m – 1116.05 m). Abundances of *T. patulus* (thin) and *P. liasicus liasicus* show an overall discontinuous trend, varying between absent and R. *Tubirhabdus patulus* (thick) was observed only sporadically as single specimens in a few samples within the lower part of its range (turneri AZ to raricostatum AZ) and occurs more consistently with R abundances

in the upper part of its range (raricostatum AZ to davoei AZ). *Crepidolithus crassus* shows an overall similar trend with variations between S and R, and an interval of frequent occurrences in the ibex AZ (1066.75 m – 1043.91 m).

Within the Mochras core, *M. lenticularis* appears as rare and is almost continuously observed until 1160.86 m (jamesoni AZ), after which its abundance decreases and specimens are only noted as VR or S. *Parhabdolithus robustus* shows a discontinuous trend of VR occurrences but shifts to R at the jamesoni/ibex AZs boundary (1116.05 m – 1121.38 m). Throughout the core, *M. jansae* appears mainly sporadic, but with a major shift to frequent occurrences at 1223.92 m (jamesoni AZ). *Similiscutum cruciulus* is observed with VR and S occurrences, with a punctual increase to rare occurrences (1106.27 m, ibex AZ), then returning to sporadic and rare occurrences.

The average absolute abundance of the total coccolith assemblage is 51.6 N/g $\times$ 10^6 (Fig. 4). Identified coccolith species were first documented at the angulata/bucklandi AZs boundary at 1739.19 m – 1753.77 m (Fig. 4 and Table 1), with the FOs of *P. liasicus* s.l. (low confidence), *M. elegans* (high confidence) and *C. primulus* (medium confidence). Through the Lower Sinemurian, several FOs are observed (Fig. 4 and Table 1), namely that of *P. liasicus distinctus* (1731.67 m – 1735.83 m; low confidence), *P. marthae* (1676.10 m – 1688.87 m; high confidence), *C. pliensbachensis* (1593.09 m – 1611.88 m; low confidence), *T. patulus* (thin) (1581.73 m – 1593.09 m; medium confidence) and *P. liasicus liasicus* (1557.45 m – 1569.52 m; medium confidence). Within this interval at 1581.73 m – 1593.09 m, the LO of *P. marthae* (high confidence) has been located (Fig. 4 and Table 1).

In the middle part of the Sinemurian, within the obtusum AZ, we denote the FCO of *P. liasicus* s.l. (1467.99 m – 1473.35 m; high confidence) and *P. liasicus distinctus* (1467.99 m – 1473.35 m; high confidence), as well as the FO of *Tubirhabdus patulus* (thick) (1461.52 m – 1467.99 m; low confidence) (Fig. 4 and Table 1). Over a long-term interval covering the Sinemurian/Pliensbachian boundary, several changes in absolute abundances, as well as FOs and LOs have been identified. From the oxynotum AZ to the Lower Pliensbachian, the base increase of *M. elegans* (1335.86 m – 1338.45 m; high confidence), the FOs of *Crepidolithus crassus* and small *Crepidolithus crassus* (1330.05 m – 1335.86; medium confidences), *M. lenticularis* (1303.73 m – 1318.26 m; high confidence), *P. robustus* (1282.60 m – 1291.36 m; low confidence), *M. jansae* (1273.63 m – 1282.60, 60 m; low confidence), and the FCOs of *C. crassus* (1303.73 m – 1318.26 m; high confidence) and *C. pliensbachensis* (1250.85 m – 1261.36 m; high confidence) have been recognized (Fig. 4 and Table 1).

Within the Lower Pliensbachian, the FOs of *M. protensa* (1248.51 m – 1250.85 m; low confidence), *C. crucifer* (1202,00 m- 1210.82 m; medium confidence), *C.* cf. *C. cantabriensis* (1147.60 m – 1152.22 m; low confidence), *C. granulatus* (thin-walled and thick-walled) (1123.34 m- 1138.10 m; low confidences), *S. cruciulus* (1123.34 m – 1138.10, 10 m; medium confidence), and of *S. avitum* (1106.27 m – 1116.05 m; low confidence) have been identified (Fig. 4 and Table 1). Furthermore, the LOs of *P. robustus* (1085.77 m – 1094.56 m; high confidence) and *C. pliensbachensis* (1106.27 m – 1116.05 m; medium confidence), the FCOs of small *C. crassus* (1241.40 m – 1248.51 m; high confidence) and of *T. patulus* (thick) (1202.00 m – 1210.82 m; high confidence) were recognized. Four major changes in absolute abundance, base and top of acme events of *M. lenticularis* (base: 1241.40 m – 1223.92 m, top: 1193.19 m – 1160.86 m; high confidences) and *C. crassus* (base: 1075.28 m – 1066.75 m, top: 1043.91 m – 1039.72 m; high confidences), have been delineated (Fig.4 and Table 1).

Discussion

Reliability of biohorizons and biozones

Numerous biohorizons have been recorded in the Mochras core, of which several species show discontinuous and sporadic occurrence that potentially affects their reliability. *Crucirhabdus primulus* is one of the three first identified species in the Mochras core. The confidence in its FO can however be considered as low, due to its sporadic record of occurrence (Figs 3, 4). Moreover, Demangel *et al*. (2020) observed this taxon already in the Rhaetian and, therefore, its FO in Mochras rather marks a stratigraphical level at which coccoliths become consistently present in the core. Perhaps, it indicates a level of flooding, which would match the trend towards more argillaceous lithology just above the Hettangian/Sinemurian boundary (Fig. 4) (Hallam 1997).

The confidence level of *M. elegans* is defined as high because specimens occur continuously throughout the whole section above this FO (Fig. 4). The FO of *P. liasicus* at the base of bucklandi AZ is considered with a low confidence, as after their FOs, specimens of *P. liasicus* s.l., as well as of *P. liasicus distinctus* show sporadic occurrences and are only rarely observed until 1467.99 m at the turneri/obtusum AZs boundary, where their FCO is marked (Fig. 4). This level

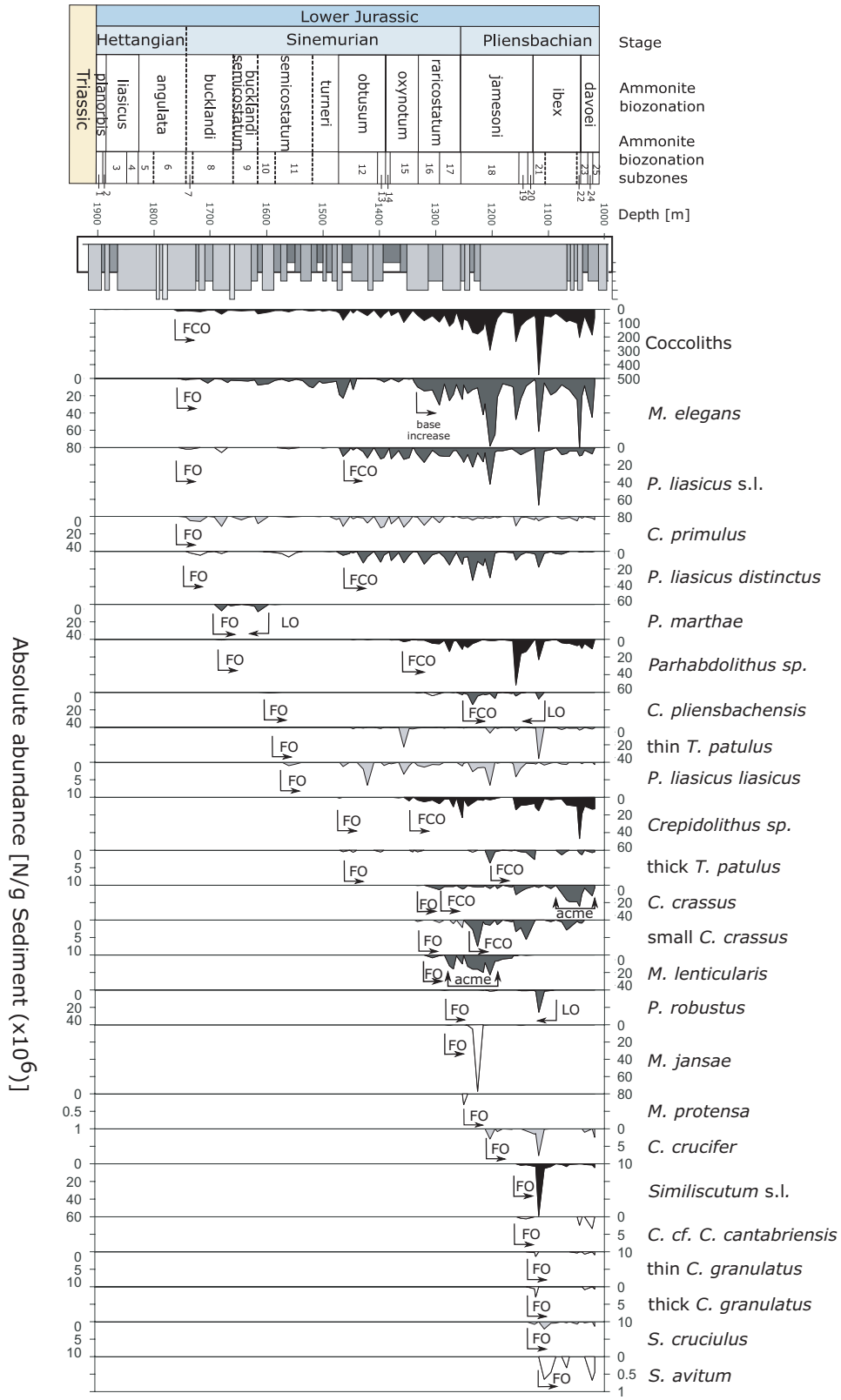

Fig. 4. Absolute abundance of coccolith species in the Hettangian to Lower Pliensbachian of the Mochras core. Black- indicating total assemblage of coccoliths, as well as genus groups of specimens with no further identification. Dark grey: species with high level of confidence. Light grey: medium level of confidence. White: low level of confidence. FO indicates the first occurrence of the species. LO represent the last occurrence of the species. FCO represent the first consistent occurrence of a species.

Table 1. Calcareous nannofossil bioevents recorded in this study calibrated to ammonite zones and subzones and their reliability or level of confidence. Top and bottom depth, as well as average age with uncertainty, derived from the astronomical age model of Storm et al. (2020). The newly proposed zonation scheme of this work (NJB), will be discussed later in the text.

Nannofossil bioevents	Stage	Ammonite Zone	Ammonite Subzone	Top depth (m)	Bottom depth (m)	Relative average age (My)	Age (Ma)	Confidence	NJB Zones	NJB Subzones
Top acme *C. crassus*	Pliensbachian	ibex	–	1039.72	1043.91	10.62 ± 0.03	188.5	High	NJB4	4b
Base acme *C. crassus*	Pliensbachian	ibex	–	1066.75	1075.28	9.95 ± 0.11	189.1	High		
LO *P. robustus*	Pliensbachian	ibex	–	1085.77	1094.56	9.54 ± 0.07	**189.6**	High		
FO *S. avitum*	Pliensbachian	ibex	–	1106.27	1116.05	9.29 ± 0	189.9	Low		
LO *C. pliensbachensis*	Pliensbachian	ibex	–	1106.27	1116.05	9.29 ± 0	189.9	Medium		4a
FO *S. cruciulus*	Pliensbachian	jamesoni	jamesoni	1123.34	1138.1	8.87 ± 0.13	**190.2**	Medium		
FO *C. granulatus* (thick-walled)	Pliensbachian	jamesoni	brevispina	1123.34	1138.1	8.87 ± 0.13	190.2	Low	NJB3	3c
FO *C. granulatus* (thin-walled)	Pliensbachian	jamesoni	brevispina	1123.34	1138.1	8.87 ± 0.13	190.2	Low		
LO *M. lenticularis*	Pliensbachian	Jamesoni	brevispina	1138.1	1142.64	8.87 ± 0.13	190.4	Medium		
FO *C.* cf. *C. cantabriensis*	Pliensbachian	jamesoni	taylori–polymorphus	1147.6	1152.22	8.54 ± 0.04	190.6	Low		3b
LO *M. jansae*	Pliensbachian	jamesoni	taylori–polymorphus	1147.6	1152.22	8.54 ± 0.04	190.6	Low		
Top acme *M. lenticularis*	Pliensbachian	jamesoni	taylori–polymorphus	1193.19	1160.86	8.01 ± 0.33	**191.1**	High		
FCO *T. patulus* (thick)	Pliensbachian	jamesoni	taylori–polymorphus	1202	1210.82	7.40 ± 0.10	191.7	High		
FO *C. crucifer*	Pliensbachian	jamesoni	taylori–polymorphus	1202	1210.82	7.40 ± 0.11	191.7	Medium		
Base acme *M. lenticularis*	Pliensbachian	jamesoni	taylori–polymorphus	1241.4	1248.51	6.64 ± 0.06	**192.5**	High		
FCO small *C. crassus*	Pliensbachian	jamesoni	taylori–polymorphus	1241.4	1248.51	6.64 ± 0.06	192.5	High		
FO *M. protensa*	Pliensbachian	jamesoni	macdonnelli–aplanatum	1248.51	1250.85	6.56 ± 0.02	192.5	Low		
FCO *C. pliensbachensis*	Sinemurian	raricostatum	macdonnelli–aplanatum	1250.85	1261.36	6.47 ± 0.07	192.6	High		3a
FO *M. jansae*	Sinemurian	raricostatum	macdonnelli–aplanatum	1273.63	1282.6	6.19 ± 0.06	192.9	Low		
FO *P. robustus*	Sinemurian	raricostatum	densinodulum–raricostatum	1282.6	1291.36	6.08 ± 0.06	193.0	Low		
FCO *C. crassus*	Sinemurian	raricostatum	densinodulum–raricostatum	1303.73	1318.26	5.73 ± 0.09	193.3	High		
FO *M. lenticularis*	Sinemurian	raricostatum	densinodulum–raricostatum	1303.73	1318.26	5.79 ± 0.14	**193.3**	High		

(*Continued*)

Table 1. (*Continued*)

Nannofossil bioevents	Stage	Ammonite Zone	Ammonite Subzone	Top depth (m)	Bottom depth (m)	Relative average age (My)	Age (Ma)	Confidence	NJB Zones	NJB Sub-zones
Base increase *M. elegans*	Sinemurian	raricostatum	densinodulum–raricostatum	1330.05	1335.86	5.42 ± 0.05	193.7	High	NJB2	2d
FO *C. crassus*	Sinemurian	raricostatum	densinodulum–raricostatum	1330.05	1335.86	5.42 ± 0.05	193.7	Medium		
FO small *C. crassus*	Sinemurian	raricostatum	densinodulum–raricostatum	1330.05	1335.86	5.42 ± 0.05	193.7	Medium		
FO *T. patulus* (thick)	Sinemurian	obtusum	obtusum–stellare	1461.52	1467.99	3.57 ± 0.05	195.5	Low		2c
FCO *P. liasicus* s.l.	Sinemurian	obtusum	obtusum–stellare	1467.99	1473.35	3.48 ± 0.04	195.6	High		
FCO *P. liasicus distinctus*	Sinemurian	obtusum	obtusum–stellare	1467.99	1473.35	3.48 ± 0.04	**195.6**	High		
FO *P. liasicus liasicus*	Sinemurian	semicostatum	scipio-nianum	1557.45	1569.52	2.19 ± 0.08	196.9	Medium		
LO *P. marthae*	Sinemurian	semicostatum	scipio-nianum	1581.73	1593.09	2.03 ± 0.08	**197.2**	High		
FO *T. patulus* (thin)	Sinemurian	semicostatum	scipio-nianum	1581.73	1593.09	1.88 ± 0.06	197.2	Medium		2b
FO *C. pliensbachensis*	Sinemurian	semicostatum	scipio-nianum	1593.09	1611.88	1.73 ± 0.09	197.4	Low		
FO *P. marthae*	Sinemurian	bucklandi	rotiforme	1676.1	1688.87	0.79 ± 0.08	**198.3**	High		
FO *P. liasicus distinctus*	Sinemurian	bucklandi	rotiforme	1731.67	1735.83	0.11 ± 0.03	199.0	Low		
FO *P. liasicus* s.l.	Sinemurian	bucklandi	conybeari	1739.19	1753.77	-0.07 ± 0.09	199.2	Low		2a
FO *C. primulus*	Sinemurian	bucklandi	conybeari	1739.19	1753.77	-0.07 ± 0.9	199.2	Medium		
FO *M. elegans*	Sinemurian	bucklandi	conybeari	1739.19	1753.77	-0.07 ± 0.9	**199.2**	High		

coincides with the FCO of coccoliths in the core and the FOs of *C. primulus* and *M. elegans*. Once again, the coincidence of all these biohorizons may be interpreted as a response to flooding.

However, interestingly, we note that the FO of *P. liasicus* specimens matches with the observations made by Mattioli & Erba (1999) in the Tethyan realm, marking the top of NJ1 and NJT1 Calcareous nannofossil zones (CNZs), respectively, at the tops of both the Hettangian stage and the angulata AZ. This level correlates with the major transgression of the top Hettangian (Haq 2018), which was perhaps responsible for a significant environmental change at the scale of the whole Peri-Tethys domain that favoured the flourishing of new coccolith species as well as their more consistent abundance. We also note a poorly reliable but distinct level of FO of *P. liasicus liasicus* at the base of semicostatum AZ, while the older FO of *P. liasicus distinctus* corresponds to that of *P. liasicus* s.l. (Fig. 4). Also, the younger FO of *P. liasicus liasicus* corresponds to the FCO of P. liasicus s.l., suggesting that the sudden increase in abundance of *P. liasicus* s.l. was caused by the origination and rapid increase of the new sub-species *P. liasicus liasicus*.

The FO of *C. pliensbachensis* is reported in the bucklandi/semicostatum AZs boundary. Its confidence level is regarded as low, due to a long absence of this taxon through the Sinemurian and reoccurrence at the oxynotum/raricostatum AZs boundary, where its FCO has been reported (Fig. 4). The FCO of *C. pliensbachensis*, however, can be defined as high in confidence level, while its LO is considered as medium, due to preceding sporadic occurrences. The FO of *T. patulus* (thin-walled) is considered as medium in terms of confidence, because of its sporadic occurrence through the section (Fig. 4). However, for the upper part of the studied section, a more continuous pattern is observed allowing the

recognition of its FCO at 1094.56 m, within the ibex AZ (Fig. 4).

After the FO of *T. patulus* (thick-walled), a discontinuous pattern is observed through the whole section, and, therefore, its confidence level is considered as low (Fig. 4). According to Bown & Cooper (1998), the LO of *P. marthae* marks the boundary between NJ2a and NJT2b calcareous nannofossil subzones (CNSzs) in the Boreal realm. We can consider both the FO and LO of *P. marthae*, as high in confidence, because this taxon does only occur during a short interval in the Lower Sinemurian, with a continuous and consistent record (Fig. 4). In addition, the morphological shape of *P. marthae* is easy to recognize, further supporting it as a robust marker for the NJ2b CNSz, herein. The FO of *C. crassus* in the top of oxynotum AZ, which marks the base of the NJ3 CNZ in NW Europe (Bown & Cooper 1998) and the NJT3 CNZ in the Tethyan realm (Mattioli & Erba 1999), is herein considered as medium in confidence level, because even though it is observed continuously above its FO and shows high abundances throughout the Mochras core, specimens of *Crepidolithus* sp. (hence possibly the same species) were already observed much earlier at the turneri/obtusum AZs boundary (1467.99 m).

Due to preservation issues, no further identification was possible on the observed *Crepidolithus* sp. specimens; so, we cannot exclude the presence of *C. crassus* already at 1467.99 m. However, the FCO of *C. crassus* was observed at 1303.731 m, with a high level of confidence and this position is just a few meters above the FO of this species, within the basal raricostatum AZ (Fig. 4). For these reasons, we suggest here that this FCO might constitute a more reliable biohorizon for marking the base of NJ3/NJT3 than its FO. Furthermore, a short-term acme event was identified for *C. crassus* between 1075.28 m and 1039.72 m, at the top part of the core, with a high level in confidence (Fig. 4).

Next to the normal sized *C. crassus*, smaller specimens of this taxon have been recognized, namely small *C. crassus*. The FO of these forms is located at the same depth as its larger relative, and considered as medium in confidence, because of their sporadic pattern (Fig. 4). The FCO of small *C. crassus*, is documented at 1241.40 m in the jamesoni AZ. The FO of *M. lenticularis* has a high level of confidence (Fig. 4). The LO of *M. lenticularis* within the studied samples can be considered as medium in confidence because of its extremely low abundance. This taxon has not been identified up-section, even though, it has been found within the margaritatus AZ samples of the same Mochras Farm (Llanbedr) borehole (Fraguas *et al.* work in progress) and in other basins around the World (e.g. Peti *et al*. 2017; Reggiani *et al*. 2010; Fraguas *et al*. 2015, 2018). Nevertheless, because of the high confidence observed for the acme event of *M. lenticularis* between 1241.400 m and 1160.86 m, based upon its relatively short range (Fig. 4), we consider that the base and top acme of *M. lenticularis* constitute robust markers for biozonation in the Mochras core.

The level of confidence of the FO of *P. robustus* is here referred as low, because specimens are only observed with discontinuous patterns throughout the section (Fig. 4). The LO of *P. robustus*, however, is considered as high in confidence, since occurrences preceding this biohorizon are consistent. Nevertheless, since specimens of *P. robustus* are rather rare in the Mochras core and its FO is low in confidence, this taxon is not considered here as a reliable marker. For *M. jansae*, both its FO and LO are considered as low in confidence. Even though we observe a distinctive pattern with a rise in abundance for two samples in the lower part of the jamesoni AZ, it is not statistically significant to be considered an acme event (Fig. 4). The LO of *M. jansae* in the upper part of the studied interval, is not considered significant and could be due to its rarity in Mochras, as it has been found in other localities up until the Early Toarcian (e.g. Mattioli & Pittet 2004; Tremolada *et al*. 2005; Fraguas *et al*. 2012, 2021; Mattioli *et al*. 2013; Ferreira *et al*., 2019; Casellato & Erba, 2015; Peti *et al*. 2017; Visentin & Erba, 2021; Visentin *et al*. 2023).

The FO of *C. crucifer* is here considered as medium in terms of confidence, because of the overall sporadic and fluctuating pattern of this taxon (Fig. 4). Specimens of *C.* cf. *C. cantabriensis* show a low level in confidence in its FO, because of its rare occurrence and discontinuous pattern throughout the studied time interval (Fig. 4). A low level in confidence is also referred to specimens of *C. granulatus* (both, thin-and thick-walled), since both are only observed rarely, showing discontinuous patterns (Fig. 4). Even though specimens of *M. protensa* were considered as significant biomarkers for the raricostatum AZ in Peti *et al*. (2017), and added as a new biomarker for NJT3c in Ferreira *et al*. (2019), herein *M. protensa* was only observed in one sample and, therefore, it cannot be considered as a robust marker for the Boreal realm. Still, it has to be noted that in Mochras, the lowest specimens of *Similiscutum* do not mark the FO of bi-shielded placolith coccoliths, since the sole occurrence of *M. protensa* precedes that of *Similiscutum*, as it was observed in the Sancerre-Couy core and in the southern peri-Tethys (Peti *et al*. 2017; Mattioli *et al*. 2013).

The FO of *S. cruciulus* is regarded as medium in confidence, because of its low abundance in the Mochras core (Fig. 4). However, when looking at the

FO *Similiscutum* s.l., which refers to either *S. cruciulus* or *S. avitum*, the confidence level can be considered as high, since specimens of *Similiscutum* are observed continuously. Even though it is still unclear how the placolith morphology did first occur or from which ancestor it evolved on (Bown 1987), the opening of the Hispanic corridor prior to the Early Pliensbachian, might have played a role in the rapid radiation of placolith coccoliths that immediately follows the FO of *Similiscutum*, as previously suggested by several authors (Plancq *et al.* 2016; Wiggan *et al.* 2018; Ferreira *et al.* 2019). The last FO recorded in the Mochras core is marked by specimens of the taxon *S. avitum*, with a low level in confidence, due to the rare and discontinuous pattern (Fig. 4).

New calcareous nannofossil zonation for the Boreal realm (NW peri-Tethys)

Ammonite biostratigraphy of the Mochras core refers to the most recent study of Storm *et al.* (2020). A detailed summary at zonal and sub-zonal levels is provided in Ivimey-Cook (1971) and Copestake & Johnson (2014). The revised biozonation is named NJB standing for the Boreal domain of the peri-Tethys (NW Europe), and in order to differentiate from the original NJ zonation established by Bown & Cooper (1998). Overall, 25 nannofossil reliable (medium-high level of confidence) biohorizons have been defined, spanning the Hettangian to Lower Pliensbachian time interval (Table 1). Examination of the reliability of these biohorizons leads us to propose new potential subzones and to revise the definition of the classic NJ zones (Fig. 5).

NJB1 – Schizosphaerella spp. CNZ

Author:- based on Bown (1987), emended herein

Definition:- from the FO of *Schizosphaerella* spp. to the FO of *Mitrolithus elegans*.

Age:- Hettangian (spans planorbis to angulata AZs)

Comments:- Equivalent to the originally defined NJ1 CNZ of Bown *et al.* (1987), this zone ranges from the FO of *Schizosphaerella* spp. to the FO of *M. elegans*. NJ1CNZ was originally named after the FO of *Schizosphaerella* spp. specimens, but very early occurrences of *Schizosphaerella* into the latest Triassic have been claimed (Clémence *et al.* 2010) and the FO of the group also precedes that of the base Hettangian ammonite marker species *Psiloceras spelae* at the Global Stratotype Section and Point (GSSP) of Kujhoch (Hillebrandt *et al.* 2013). However, both at the GSSP and in the Mochras core, a very clear feature of the base Hettangian is the consistent presence of *Schizosphaerella* spp. dominating the nannofossil

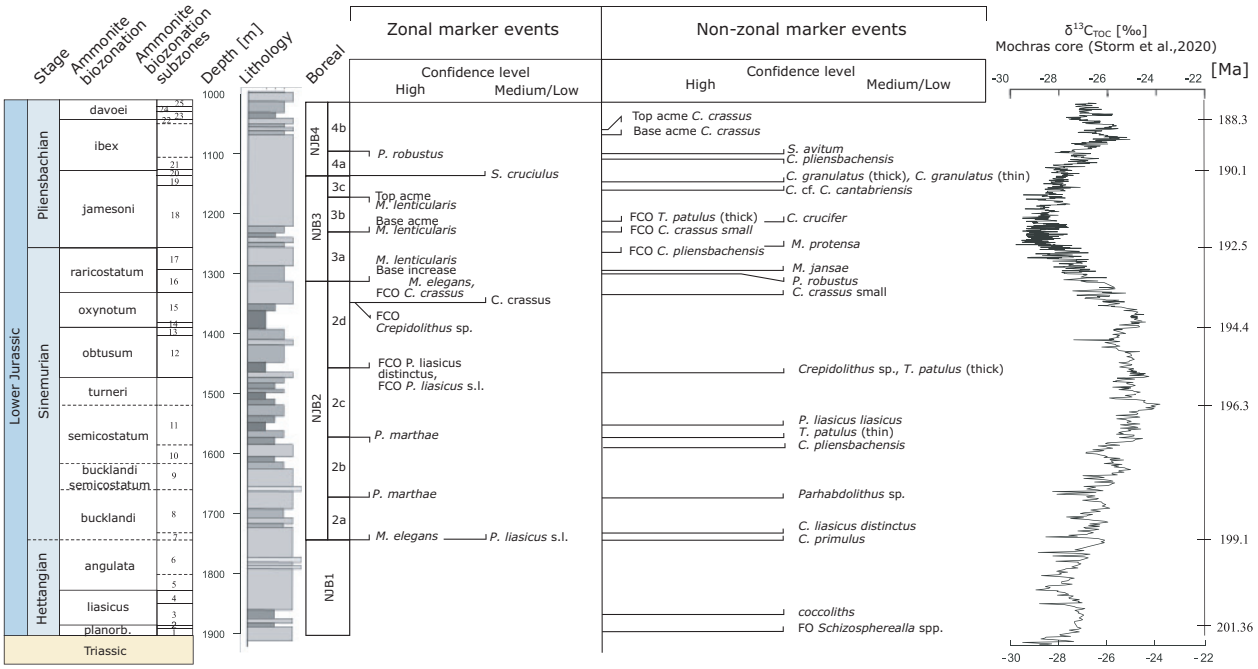

Fig. 5. New NJB calcareous nannofossil zonation, showing the suggested zonal marker bioevents and their level of confidence, as well as the non-zonal marker events of this study together with their level of confidence, on the right column, and finally the $\delta^{13}C_{TOC}$ of the Mochras core, from Storm *et al.* (2020).

assemblage. Within this zone, no significant coccolith species occur except for some poorly preserved, unidentified coccoliths and nannoliths. The coincident FOs of *C. primulus, P. liasicus* s.l. and *M. elegans* at 1739.19 m approach the position for the top of this first Jurassic CNZ. Bown (1987) chose the FO of *P. liasicus* to define the top of this zone, but also documented a coincident FO of *M. elegans*. We demonstrate here that the FO of *M. elegans* is a reliable biohorizon, showing high consistency above its FO, contrary to that of *P. liasicus*.

NJB2 – Mitrolithus elegans *CNZ*

Author:- defined herein

Definition:- from the FO of *Mitrolithus elegans* to the FO of *Mitrolithus lenticularis*

Age:- Sinemurian (from bucklandi to the base raricostatum AZs)

Comments:- This zone is named after the FO of *M. elegans*. Even though the definition of this zone differs much from that of NJ2 CNZ (Bown 1987), their stratigraphical range is close, with a similar base at the base of bucklandi AZ (base Sinemurian), while the top of NJB2 CNZ is in base raricostatum AZ instead of within the oxynotum AZ for the NJ2 CNZ of Bown (1987). The newly established CNZ is supported by the good reliability of the two chosen biohorizons, in contrast to the demonstrated low reliability of the FO of *P. liasicus* and *C. crassus* chosen by Bown (1987) to define the base and top of the NJ2 CNZ. This zone includes the successive biohorizons: FO of *C. primulus*, FO of *P. liasicus distinctus*, FO of *P. marthae*, FO of *C. pliensbachensis*, LO of *P. marthae*, FO of *P. liasicus liasicus*, FCO of *P. liasicus distinctus* and FOs of *C. crassus* and *C. crassus* small.

NJB2a – Parhabdolithus liasicus *Subzone*

Author:- defined herein

Definition:- from the FO of *Mitrolithus elegans* to the FO of *Parhabdolithus marthae*

Age:- Early Sinemurian (bucklandi AZ)

Comments:- This subzone is named after the FO of *P. liasicus* s.l. which takes place around the base of bucklandi Az but with inconsistent occurrences. The FO of *C. primulus* was recorded at the base and the FO of *P. liasicus distinctus* within this subzone. This subzone corresponds to the lower half of NJ2a CNSz of Bown & Cooper (1998) and lower half of NJT2 CNZ of Mattioli & Erba (1999).

NJB2b – Parhabdolithus marthae *Subzone*

Author:- defined herein

Definition:- from the FO of *Parhabdolithus marthae* to the LO of *Parhabdolithus marthae*

Age:- Early Sinemurian (bucklandi to lower part of the semicostatum AZs)

Comments:- This subzone is named after the full stratigraphical range of *P. marthae*. This subzone corresponds to the upper half of NJ2a CNSz of Bown & Cooper (1998), and to the upper half of NJT2 CNZ and lowermost part of NJT3 CNZ of Mattioli & Erba (1999). Although *P. marthae* is not a common species, it is easily distinguishable from *P. liasicus*, due to its recognisable robust spine. Furthermore, its short stratigraphical range and consistent record makes it a strong reliable biostratigraphical marker of the Lower Sinemurian. The FO of *C. pliensbachensis* is recorded in the topmost part of this subzone.

NJB2c – Tubirhabdus patulus *Subzone*

Author:- defined herein

Definition:- from the LO of *P. marthae* to the FCO of *P. liasicus distinctus*

Age:- Mid Sinemurian (semicostatum to lower part of obtusum AZs)

Comments:- The subzone is named after the species *Tubirhabdus patulus* due to two biohorizons recorded within the subzone for this lineage: the FO of thin-walled *T. patulus* took place around the base of this subzone, while the FO of thick-walled *T. patulus* occurred in coincidence with the FCO of *P. liasicus distinctus*. The FO of *P. liasicus liasicus* is noted in the lowermost part of this subzone while the FCO of *P. liasicus* s.l. (specimens that could not be identified at the subspecies level) also coincides with the FCO of *P. liasicus distinctus*, thus marking a significant increase in abundance of the *P. liasicus* lineage.

NJB2d – Crepidolithus crassus *Subzone*

Author:- defined herein

Definition:- from the FCO of *P. liasicus distinctus* to the FO of *M. lenticularis*

Age:- Late Sinemurian (obtusum to lower part of raricostatum AZs)

Comments:- The subzone is named after the FO of *C. crassus* that took place within this interval while the top of the subzone also coincides with the FCO of

C. crassus. Another noticeable biohorizon is the base increase of *M. elegans* that coincides with the FO of *M. lenticularis*.

NJB3 – Mitrolithus lenticularis *CNZ*

Author:- defined herein

Definition:- from the FO of *M. lenticularis* to the FO of *S. cruciulus*

Age:- Late Sinemurian (raricostatum AZ) to Early Pliensbachian (jamesoni AZ)

Comments:- This zone is named after the species *M. lenticularis*, contributing to three biohorizons recorded within this zone: the FO of *M. lenticularis* located at its base, while the acme event of this species is marking the base of the first two subzones. Even though the definition of the base of this zone differs to that of the original NJ3 CNZ of Bown (1987), the defining species at its top (*S. cruciulus*) is the same. The stratigraphical range of NJB3 CNZ is similar to NJ3 CNZ, whose base is located within the Upper Sinemurian (Lower raricostatum AZ), but with a top of NJB3 in the Lower Pliensbachian (top jamesoni AZ). The new definition is supported by the good reliability of *M. lenticularis*, instead of the demonstrated low reliability of *C. crassus*. This zone includes the successive biohorizons: FO of *M. lenitcularis*, base increase of *M. elegans*, FO of *P. robustus,* FO of *M. jansae,* FCO of *C. pliensbachensis,* FCO of *C. crassus* small, base acme of *M. lenticularis,* FO of *C. crucifer,* FCO of *T.cpatulus (thick),* top acme of *M. lenticularis,* FO of *C.* cf. *C. cantabriensis,* FO of *C. granulatus* (thick) and FO of *C. granulatus* (thin).

NJB3a – Crepidolithus pliensbachensis *subzone*

Author:- defined herein

Definition:- from the FO of *M. lenticularis* to the base acme event of *M. lenticularis*

Age: Late Sinemurian (raricostatum AZ) to Early Pliensbachian (jamesoni AZ)

Comments:- This zone is named after the FCO of *C. pliensbachensis*, within this subzone. The stratigraphical range corresponds partially to NJT3b of the Tethyan realm (Ferreria *et al.*, 2019). Other noticeable biohorizons include: FO of *P. robustus*, FO of *M. jansae* and FO of *M. protensa*.

NJB3b – Mitrolithus lenticularis *subzone*

Author:- defined herein

Definition:- from the base acme event of *M. lenticularis* to the top acme event of *M. lenticularis*

Age:- Early Pliensbachian (jamesoni AZ)

Comments:- This zone is named and defined after the recognizable acme event of *M. lenticularis*. This zone includes the FO of *C. crucifer* and the FCO of *T. patulus* (thick).

NJB3c – Crepidolithus granulatus *subzone*

Author:- defined herein

Definition:- from the top acme event of *M. lenticularis* to the FO of *S. cruciulus,*

Age:- Early Pliensbachian (jamesoni AZ)

Comments:- This subzone is named after the FO of *C. granulatus* (both, thick and thin walled) within this subzone. The subzone corresponds to the upper part of the NJ3 CNZ of Bown & Cooper (1998) and the NJT3 CNZ of Ferreira *et al.* (2019). Additional biohorizons include: FO of *C.* cf. *C. cantabriensis,* LO of *M. lenticularis* and FO of *S. cruciulus.*

NJB4 – Similiscutum cruciulus *CNZ*

Author:- Bown (1987), emended herein

Definition:- from the FO of *S. cruciulus* to the FO of *Lotharingius hauffii*

Age:- Pliensbachian (jamesoni AZ to margaritatus AZ)

Comments:- This zone is named after the FO of *S. cruciulus.* The top of this zone (FO of *L. hauffii*) was not observed, as this study investigated only until the lower part of the davoei AZ. However, *L. hauffii* is a species consistently found within the margaritatus AZ (Bown 1987; Bown & Cooper 1998; Fraguas *et al.* 2015, 2018; Peti *et al.* 2017; Ferreira *et al.* 2019) or spinatum AZ (Mattioli & Erba 1999; Mattioli *et al.* 2013). This zone includes the successive biohorizons: LO of *C. pliensbachensis*, FO of *S. avitum*, LO of *P. robustus*, base acme of *C. crassus* and top acme of *C. crassus*.

NJB4a – Parhabdolithus robustus *subzone*

Author:- Bown (1987), emended herein

Definition:- from the FO of *S. cruciulus* to the LO of *P. robustus*

Age:- Early Pliensbachian (jamesoni AZ to ibex AZ)

Comments:- This subzone is named after the LO of *P. robustus* and is equivalent to NJ4a of Bown

(1987). Additional biohorizons within this subzone include the LO *C. pliensbachensis* and the FO of *S. avitum*.

Comparison to previous Tethyan and peri-Tethyan realm nannofossil zonations

Calcareous nannofossil occurrences and bioevents, in this study (Boreal realm) are plotted against the results from Bown & Cooper (1998) in Fig. 6A, and those of Mattioli & Erba (1999), Peti *et al*. (2017) and Ferreira *et al*. (2019) are shown in Fig. 6B. The biostratigraphical scheme of Bown & Cooper (1998) relied very much on the original work of Bown (1987) on the Mochras core. It is therefore important to compare and analyse differences in the observed bioevents. Correlations of nannofossil bioevents and ammonite zones between different realm localities might be impaired by pronounced ammonite provincialism during the Early Jurassic (e.g. Macchioni & Cecca 2002; Dommergues *et al*. 2009; Dera *et al*. 2011). Even though apparent diachronism of nannofossil taxa between the Boreal and the peri-Tethyan realms (Figs.6A-B), may partially be affected by poor preservation or palaeoprovincialsm, bioevents bearing noticeably discrepancies between the different localities are here analysed and discussed.

Bown & Cooper (1998) placed the base of the NJ2 CNZ in the upper angulata AZ, considering the FO of *P. liasicus*, and marked a relatively long time interval for the FO of *S. punctulata*. In our study, we were able to mark more precisely the FO of *Schizosphaerella* spp within the planorbis AZ. The base of NJB2 CNZ was placed at the Hettangian/Sinemurian boundary after the FO of *M. elegans*, which in our study is slightly younger compared to Bown & Cooper (1998). The base of NJ3 CNZ was placed by Bown & Cooper (1998) close to the oxynotum/obtusum AZs boundary after the FO of *C. crassus*. In this work, the base of NJB3 CNZ was placed slightly younger in the core, within the lower part of the raricostatum AZ, after the FO of *M. lenticularis*, which showed to be more robust (Fig. 6a). The LO of *P. marthae* differentiates the NJ2a and NJ2b CNSzs in the work of Bown & Cooper (1998), while in our study, the NJB2 CNZ is subdivided based upon the FO of this species. The base as well as the new proposed subdivisions of NJB3a-cCNSzs does not correlate to any previous biozones of the Mochras core. One exception is the top of NJ3, which is located after the FO of *S. cruciulus* by Bown & Cooper (1998), and in Mochras matches to base of NJB3b defined by acme event of *M. lenticularis* (Fig. 6A). According to Bown & Cooper (1998), the base of the NJ4 CNZ is recorded in the lower part of the jamesoni AZ, whilst in our study the base of NJB4 CNZ is located in the Upper jamesoni AZ. The LO of *P. robustus*, differentiating NJ4a and NJ4b in the Lower ibex AZ, is concordant in Bown & Cooper (1998) and this study.

Comparison of our new biozones to the work of Mattioli & Erba (1999), shows a lot of differences in the FO and LO of calcareous nannofossil species. In the Mediterranean area, the base of NJT2 is defined after FO of *P. liasicus* in the liasicus AZ. However, in our study the base of NJB2 is recorded much younger at the Hettangian/Sinemurian boundary after the FO of *M. elegans*, which is shown to be a more reliable marker than *P. liasicus*. For the new proposed subdivisions of NJB2 it is noticeable that NJB2a correlates quite well with NJT2b of Mattioli & Erba (1999). Both bases are marked with the FO of *M. elegans*, however, the top of NJT2b is identified after the FO of *C. pliensbachensis* and, in Mochras, after the FO of *P. marthae*. The FO of *C. pliensbachensis* in Italy/S France also markes the base of NJT3 at the Upper bucklandi AZ (Fig. 6B), whilst in our study the base of NJB3 is identified much later in the lower raricostatum AZ after the FO of *M. lenticularis*, the base increase of *M. elegans* and the FCO of *C. crassus*. None of the new proposed subdivisions of NJB3 correlate to the biozones in Italy/S France, except of the NJB3a which corresponds well with NJT3b, highlighting a similar record of the FO of *M. lenticularis* in the Lower raricostatum AZ. Both biozonation schemes mark the base of NJB4 and NJT4 after the FO of *S. cruciulus*, however, in our study this event occurs much earlier at the jamesoni/ibex AZ boundary. The subdivision NJB4a shows a correlating record to NJT4a, both identifying the base after the LO of *P. robustus*.

When comparing the new biozones of the Mochras core, defined herein, to those from the Sancerre core (Peti *et al*. 2017), we can only compare biozones above the Hettangian to mid-Sinemurian, due to a major influence of rising sea-level during that time interval in the Paris Basin (Peti *et al*. 2017). Therefore, neither NJB1 nor NJB2 CNZs correlate with biozones identified at the Sancerre core. The base of NJB3 CNZ is defined by the LO of *P. marthae* in the lower semicostatum AZ in the Mochras core. However, in Sancerre, the LO of *P. marthae* is identified much earlier and located in an undefined interval close the jamesoni AZ (Fig. 6B). The new proposed subdivisions of NJB3a-cCNSzs do not correlate to the biozonation in the Sancerre core. However, new results on the FCO of *C. crassus* both in Mochras and in Sancerre help to approach the base of the raricostatum AZ, located at the base NJB3a CNSz in

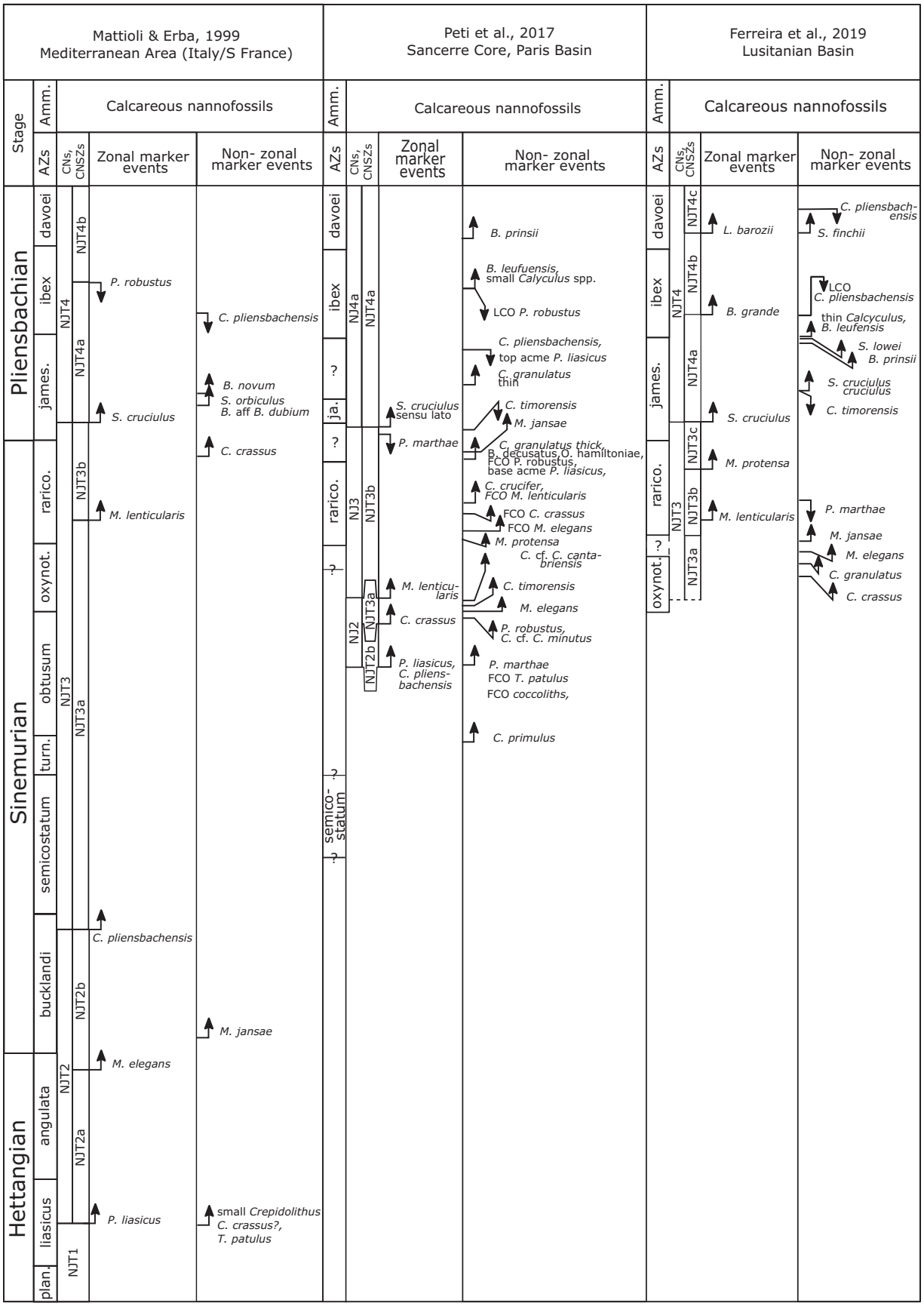
Mattioli & Erba, 1999
Mediterranean Area (Italy/S France)
Peti et al., 2017
Sancerre Core, Paris Basin
Ferreira et al., 2019
Lusitanian Basin
Stage
Amm.
Calcareous nannofossils
AZs
CNs, CNSZs
Zonal marker events
Non- zonal marker events
Pliensbachian
Sinemurian
Hettangian
davoei
ibex
james.
rarico.
oxynot.
obtusum
turn.
semicostatum
bucklandi
angulata
liasicus
plan.
NJT4
NJT4b
NJT4a
NJT3
NJT3b
NJT3a
NJT2
NJT2b
NJT2a
NJT1
P. robustus
S. cruciulus
M. lenticularis
C. pliensbachensis
M. elegans
P. liasicus
C. pliensbachensis
B. novum
S. orbiculus
B. aff B. dubium
C. crassus
M. jansae
small Crepidolithus
C. crassus?,
T. patulus
ja.
semico-statum
NJ4a
NJ3
NJ2
NJT3a
NJT2b
S. cruciulus sensu lato
P. marthae
M. lenticu-laris
C. crassus
P. liasicus, C. pliens-bachensis
B. prinsii
B. leufuensis, small Calyculus spp.
LCO P. robustus
C. pliensbachensis, top acme P. liasicus
C. granulatus thin
C. timorensis
M. jansae
C. granulatus thick, B. decusatus, O. hamiltoniae, FCO P. robustus, base acme P. liasicus,
C. crucifer, FCO M. lenticularis
FCO C. crassus
FCO M. elegans
M. protensa
C. cf. C. canta-briensis
C. timorensis
M. elegans
P. robustus, C. cf. C. minutus
P. marthae
FCO T. patulus
FCO coccoliths,
C. primulus
NJT4c
NJT3c
L. barozii
B. grande
S. cruciulus
M. protensa
M. lenticularis
C. pliensbach-ensis
S. finchii
LCO
C. pliensbachensis
thin Calcyculus, B. leufensis
S. lowei
B. prinsii
S. cruciulus cruciulus
C. timorensis
P. marthae
M. jansae
M. elegans
C. granulatus
C. crassus

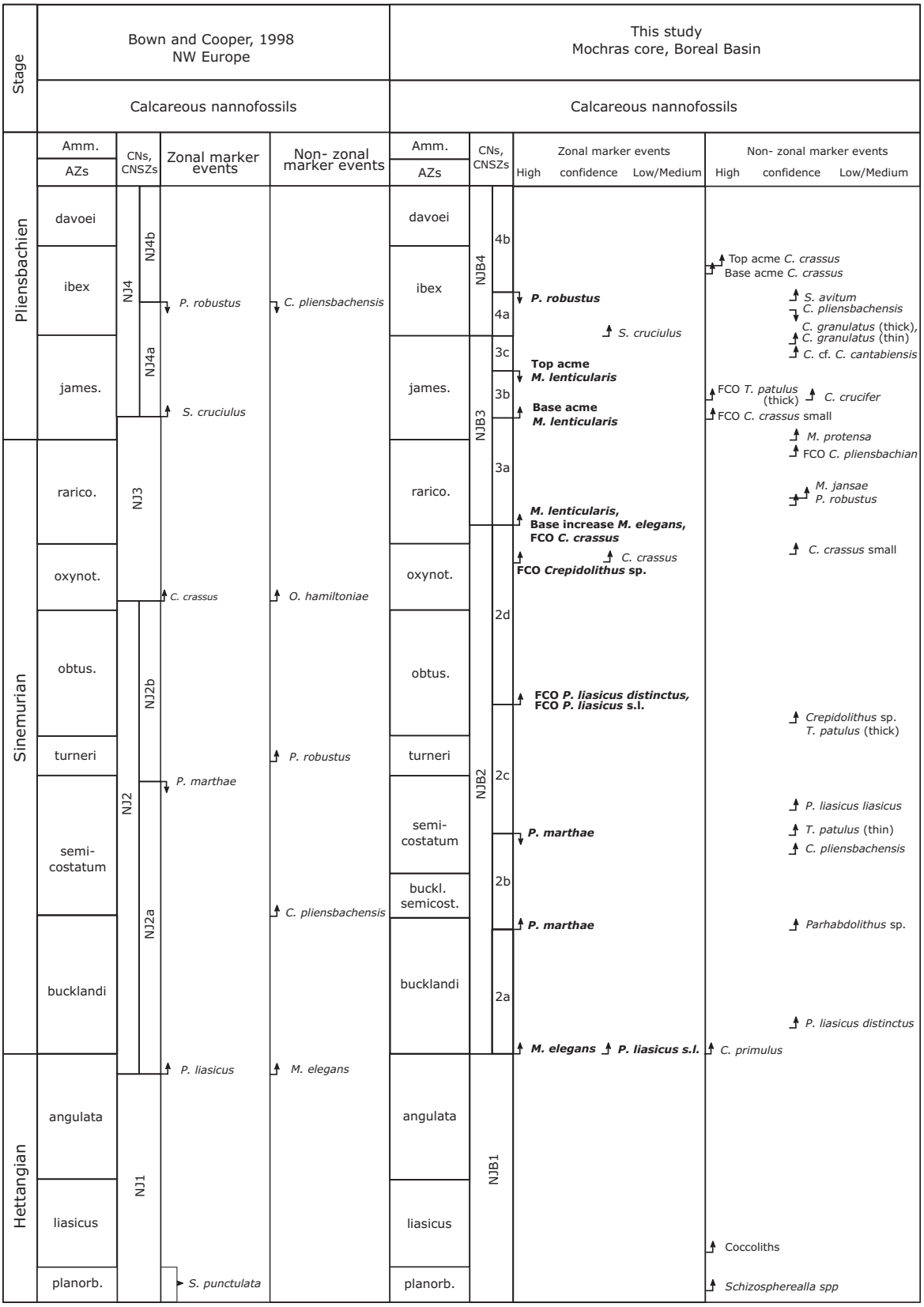

Fig. 6. A, comparison of calcareous nannofossil zonation of this study (Mochras core, Boreal Basin) with the previous Mochras study (NW Europe; Bown & Cooper 1998). B, comparison of calcareous nannofossil zonations proposed for the Mediterranean area (Mattioli & Erba, 1999), the Paris Basin (France; Peti *et al.* 2017) and Western Tethys (Lusitanian Basin; Ferreira *et al.* 2019). Ammonite zones have been correlated, respectively: Ammonites; AZs: Ammonite zones; CNZs: Calcareous nannofossil zones; CNSzs: Calcareous nannofossil subzones. Dashed lines represent uncertain positions of zone boundaries. Bold species represent proposed additional bioevents in the Mochras core.

Mochras. Because in both studies the FCO of *C. crassus* was assigned to be robust, it opens the possibility to use these more reliable non-standard biostratigraphical taxa to define this bioevents in Sancerre. The base of NJB3b CNSz in Mochras is defined by the acme event of *M. lenticularis*, located close to the raricostatum/jamesoni AZs boundary and correlates to the LO of *P. marthae* and *C. timorensis*, as well as the FO of *S. cruciulus* s.l. in an undefined interval close to the base of the NJT4 CNZ in Sancerre. Biozones of the Early Pliensbachian defined in the Mochras core, do not correlate to any biozone in Sancerre. In Mochras, the base of the NJB4 CNZ is recorded jamesoni ASz of the jamesoni AZ and thus slightly above than defined in Sancerre.

It is noteworthy that the calcareous nannofossil zonation defined by Ferreira *et al*. (2019) in the Lusitanian Basin (Western Tethys) only includes biozones from the oxynotum AZ upwards. Herein, the base of NJB3a is defined by the FO of *M. lenticularis* during the lower raricostatum AZ. The FO of this taxon correlates greatly with the results of the Lusitanian Basin (Fig. 6B), although it marks the base of the NJT3b CNSz in the Tethyan realm (Mattioli & Erba 1999; Ferreira *et al*. 2019). Thus, the new results on the level of confidence of *M. lenticularis* open the possibility to use the FO of this taxon as a reliable non-standard biostratigraphical marker in more studies. Further, both *M. protensa* and *S. cruciulus* seem to occur later in the Mochras core, compared to the Lusitanian Basin. Therefore, the onset of NJB4 CNZ is defined much later in the late jamesoni AZ, while in the Lusitanian Basin *S. cruciulus* occurred in the early jamesoni AZ (Fig. 6B). However, the onset of NJT4 CNZ in the Lusitanian Basin, correlates with the NJB3b CNSz, defined by the base acme event of *M. lenticularis*, in Mochras. Besides the definition of NJB3a and NJB3b CNSzs no further biozones defined in the Mochras core correlate to any biozone in the Lusitanian Basin.

Similarities of bioevents and secondary or non-zonal bioevents between the previous and the revised scheme of the Mochras core are represented by a correlation of the FO and LO of *C. pliensbachensis*, as well as the LO of *P. robustus*. However, no FO of *P. marthae* was recorded by Bown and Cooper (1998), which in our study is considered a main bioevent for dividing the NJB2a and NJB2b CNSzs. In our revised work, much more samples were analysed, and therefore more taxa and bioevents were identified. Additionally, we included the FCO, LCO and statistically proven acme events to consider placing robust bioevents, which makes the updated scheme highly reliable and reproducible.

Similarities of secondary bioevents or non-zonal bioevents to samples in Sancerre are represented by a change in abundance of *M. elegans* at the base raricostatum AZ. In Sancerre, this change is marked as FCO (Fig. 6B), while in Mochras we set the base increase of *M. elegans*. Another similarity is represented by the LO of *P. robustus*, which in Sancerre corresponds to the LCO of *P. robustus*. Despite the named similarities, both localities show some major differences. For instance, the timing and duration in the range of *P. marthae*. In Mochras, *P. marthae* is identified in a short time interval during the bucklandi-semicostatum to lower semicostatum AZs, while, in Sancerre, *P. marthae* seems to occur during a longer time, with its FO observed at the base of NJ2 CNZ probably during the obtusum AZ (Fig. 6B). Another dissimilarity is the observation of a pronounced increase of *C. crassus* in Mochras during the upper part of the ibex AZ, characterized as an acme event, whilst in Sancerre no such change in abundance during that time was observed. Also, no *B. leufuensis, B. prinsii* nor small *Calyculus* spp. have been identified in the Mochras core during the ibex-davoei AZs, while Peti *et al*. (2017) clearly documented the occurrence of these nannofossils during this time interval (Fig. 6B).

Conclusions

Evaluation of 26 new defined events in the Mochras core, revealed that a low abundance of many index species towards the base and top of their stratigraphical range show inconsistent records, while FCOs and LCOs as well as base and top of acme events seem to be more reliable. In this study, all nannofossil species have been tested on their reliability as level of confidence, of which nine non-zonal biomarkers have been proven to be robust. Therefore, a new zonation has been proposed with additional subzones for NJB2 (a-d) and NJB3 (a-c), defined after reliable biomarkers, which are not currently used as standard markers. Based on the new results, we updated the zonation scheme for the reference borehole of Mochras and tested the results against other localities.

Acknowledgements. – Emanuela Mattioli is acknowledged for her tremendous help following and discussing the taxonomy of the species identified throughout this study. Many thanks to an anonymous reviewer for the constructive and useful comments and also to Clemens V. Ullmann for managing, preparing and distributing sample bags of Mochras to us. This study is part of the Early Jurassic Earth System and Timescale (JET) research project.

References

Agnini, C., Fornaciari, E., Raffi, I., Catanzariti, R., Pälike, H., Backman, J. & Rio, D. 2014: Biozonation and biochronology of Paleogene calcareous nannofossils from low and middle latitudes. *Newsletters on Stratigraphy 47*, 131–181. https://doi.org/10.1127/0078-0421/2014/0042

Bassoullet, J.P. & Baudin, F. 1994: Le Toarcien inférieur: une période de crise dans les bassins et sur les plate-formes carbonatées de l'Europe du Nord-Ouest et de la Téthys. *Geobios 27*, 645–654. https://doi.org/10.1016/S0016-6995(94)80227-0

Bown, P.R. 1987: Taxonomy, Evolution, and Biostratigraphy of Late Triassic-Early Jurassic Calcareous Nannofossils. *Special Papers in Palaeontology 38*, 1–118.

Bown, P.R. & Cooper, M.K.E. 1998: Jurassic. Published in: *Calcareous Nannofossil Biostratigraphy*: British Micropalaeont, Soc. Publ. Ser., Kluever Acad. Publish, Cambridge *Calcareous Nannofossil Biostratigraphy*, 34–85. https://doi.org/10.1007/978-94-011-4902-04

Bown, P.R., Lees, J.A. & Young, J.R. 2004: Calcareous nannoplankton evolution and diversity through time. In: Thierstein, H.R & Young, J.R. (eds) *Coccolithophores*, 481–508. Springer, Berlin, Heidelberg. https://doi.org/10.1007/978-3-662-06278-4_18

Clémence, M.E., Gardin, S., Bartolini, A., Paris, G., Beaumont, V. & Guex, J. 2010: Bentho-planktonic evidence from the Austrian Alps for a decline in sea-surface carbonate production at the end of the Triassic. *Swiss Journal of Geosciences 103*, 293–315. https://doi.org/10.1007/s00015-010-0019-z

Chaumeil Rodríguez, M., Mattioli, E. & Pérez Panera, J.P. 2022: Lower Jurassic calcareous nannofossil taxonomy revisited according to the Neuquén Basin (Argentina) record. *Journal of Micropalaeontology 41*, 75–105. https://doi.org/10.5194/jm-41-75-2022

Cifer, T., Goričan, Š., Auer, M., Demény, A., Fraguas, Á., Gawlick, H.J. & Riechelmann, S. 2022: Integrated stratigraphy (radiolarians, calcareous nannofossils, carbon and strontium isotopes) of the Sinemurian–Pliensbachian transition at Mt Rettenstein, Northern Calcareous Alps, Austria. *Global and Planetary Change 212*, 103811. https://doi.org/10.1016/j.gloplacha.2022.103811

Copestake, P. & Johnson, B. 2013: Lower Jurassic Foraminifera from the Llanbedr (Mochras Farm) Borehole, North Wales, UK. *Monographs of the Palaeontographical Society 167*, 1–403. https://doi.org/10.1080/02693445.2013.11963952

Coward, M.P., Dewey, J.F., Hempton, M. & Holroyd, J. 2003: Tectonic evolution. In: Evans D., Graham C., Armour A. & Bathurst P. (eds) The Millennium Atlas: Petroleum Geology of The Central and Northern North Sea Geological Society Publishing House, London, 17–33.

Demangel, I., Kovács, Z., Richoz, S., Gardin, S., Krystyn, L., Baldermann, A. & Piller, W.E. 2020: Development of early calcareous nannoplankton in the late Triassic (Northern Calcareous Alps, Austria). *Global and Planetary Change 193*, 103254. https://doi.org/10.1016/j.gloplacha.2020.103254

Dera, G., Brigaud, B., Monna, F., Laffont, R., Pucéat, E., Deconinck, J.F., Pellenard, P., Joachimski, M.M. & Durlet, C. 2011: Climatic ups and downs in a disturbed Jurassic world. *Geology 39*, 215–218. https://doi.org/10.1130/G31579.1

Dommergues, J.L., Fara, E. & Meister, C. 2009: Ammonite diversity and its palaeobiogeographical structure during the early Pliensbachian (Jurassic) in the western Tethys and adjacent areas. *Palaeogeography, Palaeoclimatology, Palaeoecology 280*, 64–77. https://doi.org/10.1016/j.palaeo.2009.06.005

Erba, E. 2004: Calcareous nannofossils and Mesozoic oceanic anoxic events. *Marine Micropaleontology 52*, 85–106. https://doi.org/10.1016/j.marmicro.2004.04.007

Ferreira, J., Mattioli, E. & van de Schootbrugge, B. 2017: Palaeoenvironmental vs. evolutionary control on size variation of coccoliths across the Lower-Middle Jurassic. *Palaeogeography, Palaeoclimatology, Palaeoecology 465*, 177–192. https://doi.org/10.1016/j.palaeo.2016.10.029

Ferreira, J., Mattioli, E., Suchéras-Marx, B., Giraud, F., Duarte, L.V., Pittet, B., Suan, G., Hassler, A. & Spangenberg, J.E. 2019: Western Tethys early and Middle Jurassic calcareous nannofossil biostratigraphy. *Earth-Science Reviews 197*, 102908. https://doi.org/10.1016/j.earscirev.2019.102908

Fraguas, Á. 2014: *Crepidolithus cantabriensis* nov. sp., a new calcareous nannofossil (Prymnesiophyceae) from the Lower Jurassic of northern Spain. *Geobios 47*, 31–38. https://doi.org/10.1016/j.geobios.2013.10.004

Fraguas, Á. & Erba, E. 2010: Biometric analyses as a tool for the differentiation of two coccolith species of the genus *Crepidolithus* (Pliensbachian, Lower Jurassic) in the Basque-Cantabrian Basin (Northern Spain). *Marine Micropaleontology 77*, 125–136. https://doi.org/10.1016/j.marmicro.2010.08.004

Fraguas, Á. & Young, J.R. 2011: Evolution of the coccolith genus *Lotharingius* during the Late Pliensbachian-Early Toarcian interval in Asturias (N Spain). Consequences of the Early Toarcian environmental perturbations. *Geobios 44*, 361–375. https://doi.org/10.1016/j.geobios.2010.10.005

Fraguas, Á., Comas-Rengifo, M.J., Goy, A. & Gómez, J.J. 2018: Upper Sinemurian–Pliensbachian calcareous nannofossil biostratigraphy of the E Rodiles section (Asturias, N Spain): a reference section for the connection between the Boreal and Tethyan Realms. *Newsletters on Stratigraphy 51*, 227–244. https://doi.org/10.1127/nos/2017/0401

Fraguas, Á., Comas-Rengifo, M.J., Gómez, J.J. & Goy, A. 2012: The calcareous nannofossil crisis in Northern Spain (Asturias province) linked to the Early Toarcian warming-driven mass extinction. *Marine Micropaleontology 94*, 58–71. https://doi.org/10.1016/j.marmicro.2012.06.004

Fraguas, Á., Comas-Rengifo, M.J. & Perilli, N. 2015: Calcareous nannofossil biostratigraphy of the Lower Jurassic in the Cantabrian Range (northern Spain). *Newsletters on Stratigraphy 49*, 179–199. https://doi.org/10.1127/nos/2015/0059

Fraguas, Á., Gómez, J.J., Goy, A. & Comas-Rengifo, M.J. 2021: The response of calcareous nannoplankton to the latest Pliensbachian–early Toarcian environmental changes in the Camino Section (Basque Cantabrian Basin, northern Spain). *Geological Society, London, Special Publications 514*, 31–58. https://doi.org/10.1144/SP514-2020-256

Hallam, A. 1997: Estimates of the amount and rate of sea-level change across the Rhaetian—Hettangian and Pliensbachian—Toarcian boundaries (latest Triassic to early Jurassic). *Journal of the Geological Society 154*, 773–779. https://doi.org/10.1144/gsjgs.154.5.0773

Hay, W.W. 1972: Probabilistic stratigraphy. *Eclogae Geologicae Helvetiae 65*, 255–266.

Hermoso, M., Le Callonnec, L., Minoletti, F., Renard, M. & Hesselbo, S.P. 2009: Expression of the Early Toarcian negative carbon-isotope excursion in separated carbonate microfractions (Jurassic, Paris Basin). *Earth and Planetary Science Letters 277*, 194–203. https://doi.org/10.1016/j.epsl.2008.10.013

Hesselbo, S.P., Bjerrum, C.J., Hinnov, L.A., MacNiocaill, C., Miller, K.G., Riding, J.B. & Van de Schootbrugge, B. 2013: Mochras borehole revisited: a new global standard for Early Jurassic earth history. *Scientific Drilling 16*, 81–91. https://doi.org/10.5194/sd-16-81-2013

Hillebrandt, A.V., Krystyn, L., Kürschner, W.M., Bonis, N.R., Ruhl, M., Richoz, S., Schobben, M.A.N., Urlichs, M., Bown, P.R., Kment, K. & McRoberts, C.A. 2013: The global stratotype sections and point (GSSP) for the base of the Jurassic System at Kuhjoch (Karwendel Mountains, Northern Calcareous Alps, Tyrol, Austria). *Episodes 36*, pp. 162–198. https://doi.org/10.18814/epiiugs/2013/v36i3/001

Ivimey-Cook, H.C. 1971: *Stratigraphical palaeontology of the Lower Jurassic of the Llanbedr (Mochras Farm) Borehole*. HM Stationery Office, London.

Koch, C. & Young, J.R. 2007: A simple weighing and dilution technique for determining absolute abundances of coccoliths from sediment samples. *Journal of Nannoplankton Research 29*, 6–69. https://doi.org/10.58998/jnr2150

Korte, C., Hesselbo, S.P., Ullmann, C.V., Dietl, G., Ruhl, M., Schweigert, G. & Thibault, N. 2015: Jurassic climate mode governed by ocean gateway. *Nature Communications 6*, 1–7. https://doi.org/10.1038/ncomms10015

Macchioni, F. & Cecca, F. 2002: Biodiversity and biogeography of middle–late Liassic ammonoids: implications for the early Toarcian mass extinction. *Geobios 35*, 165–175. https://doi.org/10.1016/S0016-6995(02)00057-8

Mailliot, S., Mattioli, E., Chaumeil Rodríguez, M. & Pittet, B. 2023: Revisiting Early Jurassic Biscutaceae: *Similiscutum giganteum* sp. nov. *Journal of Micropalaeontology 42*, 1–12. https://doi.org/10.5194/jm-42-1-2023

Mattioli, E. & Erba, E. 1999: Synthesis of calcareous nannofossil events in Tethyan Lower and Middle Jurassic successions. *Rivista Italiana di Paleontologia e Stratigrafia 105*, 343–376.

Mattioli, E., Plancq, J., Boussaha, M., Duarte, L.V. & Pittet, B. 2013: Calcareous nannofossil biostratigraphy: new data from the Lower Jurassic of the Lusitanian Basin. *Comunicaçõe Geológicas*, *100*, 69–76.

Mattioli, E., Pittet, B., Young, J.R. & Bown, P.R. 2004: Biometric analysis of Pliensbachian-Toarcian (Lower Jurassic) coccoliths of the family Biscutaceae: intra-and interspecific variability versus palaeoenvironmental influence. *Marine Micropaleontology 52*, 5–27. https://doi.org/10.1016/j.marmicro.2004.04.004

Perilli, N., Fraguas, Á. & Comas-Rengifo, M.J. 2010: Reproducibility and reliability of the Pliensbachian calcareous nannofossil biohorizons from the Basque-Cantabrian Basin (Northern Spain). *Geobios 43*, 77–85. https://doi.org/10.1016/j.geobios.2009.06.009

Peti, L., Thibault, N., Clémence, M.E., Korte, C., Dommergues, J.L., Bougeault, C., Pellenard, P., Jelby, M.E. & Ullmann, C.V. 2017: Sinemurian–Pliensbachian calcareous nannofossil biostratigraphy and organic carbon isotope stratigraphy in the Paris Basin: Calibration to the ammonite biozonation of NW Europe. *Palaeogeography, Palaeoclimatology, Palaeoecology 468*, 142–161. https://doi.org/10.1016/j.palaeo.2016.12.004

Peti, L. & Thibault, N. 2022: Early Jurassic coccolith diversification and response to pre-Toarcian environmental changes: a perspective from the Paris Basin. *Marine Micropaleontology 177*, 102173. https://doi.org/10.1016/j.marmicro.2022.102173

Plancq, J., Mattioli, E., Pittet, B., Baudin, F., Duarte, L.V., Boussaha, M. & Grossi, V. 2016: A calcareous nannofossil and organic geochemical study of marine palaeoenvironmental changes across the Sinemurian/Pliensbachian (early Jurassic, ~191 Ma) in Portugal. *Palaeogeography, Palaeoclimatology, Palaeoecology 449*, 1–12. https://doi.org/10.1016/j.palaeo.2016.02.009

Reggiani, L., Mattioli, E., Pittet, B., Duarte, L.V., de Oliveira, L.V. & Comas-Rengifo, M.J. 2010: Pliensbachian (Early Jurassic) calcareous nannofossils from the Peniche section (Lusitanian Basin, Portugal): A clue for palaeoenvironmental reconstructions. *Marine Micropaleontology*, *75*, 1–16. https://doi.org/10.1016/j.marmicro.2010.02.002

Roth, P.H. 1983: Jurassic and lower cretaceous calcareous nannofossils in the western north-atlantic (site-534)-biostratigraphy, preservation, and some observations on biogeography and paleoceanography. *Initial Reports of the Deep Sea Drilling Project*, *76*, 587pp. https://doi.org/10.2973/dsdp.proc.76.125.1983

Ruhl, M., Hesselbo, S.P., Hinnov, L., Jenkyns, H.C., Xu, W., Riding, J.B., Storm, M., Minisini, D., Ullmann, C.V. & Leng, M.J. 2016: Astronomical constraints on the duration of the Early Jurassic Pliensbachian Stage and global climatic fluctuations. *Earth and Planetary Science Letters 455*, 149–165. https://doi.org/10.1016/j.epsl.2016.08.038

Scotese, C.R. 2016: Tutorial: PALEOMAP paleoAtlas for GPlates and the paleoData plotter program, *PALAEOMAP Project, Technical Report*, 56. https://doi.org/10.1130/abs/2016NC-275387

Storm, M.S., Hesselbo, S.P., Jenkyns, H.C., Ruhl, M., Ullmann, C.V., Xu, W., Leng, M.J., Riding, J.B. & Gorbanenko, O. 2020: Orbital pacing and secular evolution of the Early Jurassic carbon cycle. *Proceedings of the National Academy of Sciences 117*, 3974–3982. https://doi.org/10.1073/pnas.1912094117

Suchéras-Marx, B., Mattioli, E., Pittet, B., Escarguel, G. & Suan, G. 2010: Astronomically-paced coccolith size variations during the early Pliensbachian (Early Jurassic). *Palaeogeography, Palaeoclimatology, Palaeoecology 295*, 281–292. https://doi.org/10.1016/j.palaeo.2010.06.006

Tappin, D.R., Chadwick, R.A., Jackson, A.A., Wingfield, R.T.R. & Smith, N.J.P. 1994: *The Geology of Cardigan Bay and the Bristol Channel*. UK Offshore Regional report, British Geological Survey.

Thibault, N., Harlou, R., Schovsbo, N., Schiøler, P., Minoletti, F., Galbrun, B. & Surlyk, F. 2012a: Upper Campanian–Maastrichtian nannofossil biostratigraphy and high-resolution carbon-isotope stratigraphy of the Danish Basin: towards a standard δ13C curve for the Boreal Realm. *Cretaceous Research 33*, 72–90. https://doi.org/10.1016/j.cretres.2011.09.001

Thibault, N., Husson, D., Harlou, R., Gardin, S., Galbrun, B., Huret, E. & Minoletti, F. 2012b: Astronomical calibration of upper Campanian–Maastrichtian carbon isotope events and calcareous plankton biostratigraphy in the Indian Ocean (ODP Hole 762C): Implication for the age of the Campanian–Maastrichtian boundary. *Palaeogeography, Palaeoclimatology, Palaeoecology 337*, 52–71. https://doi.org/10.1016/j.palaeo.2012.03.027

Ullmann, C.V., Szűcs, D., Jiang, M., Hudson, A.J. & Hesselbo, S.P. 2022: Geochemistry of macrofossil, bulk rock and secondary calcite in the Early Jurassic strata of the Llanbedr (Mochras Farm) drill core, Cardigan Bay Basin, Wales, UK. *Journal of the Geological Society 179*, 1–17. https://doi.org/10.1144/jgs2021-018

van de Schootbrugge, B., McArthur, J.M., Bailey, T.R., Rosenthal, Y., Wright, J.D. & Miller, K.G. 2005: Toarcian oceanic anoxic event: an assessment of global causes using belemnite C isotope records. *Paleoceanography 20*, 3, Article PA3008, 1–10. https://doi.org/10.1029/2004PA001102

Veiga de Oliveira, L.V., Perilli, N. & Duarte, L.V. 2007: Calcareous nannofossil assemblages around the Pliensbachian/Toarcian boundary in the reference section of Peniche (Portugal). *Ciências da Terra/Earth Sciences Journal 16*, 45–50.

Visentin, S. & Erba, E. 2021: High-resolution calcareous nannofossil biostratigraphy across the Toarcian Oceanic Anoxic Event in northern Italy: clues from the Sogno and Gajum Cores (Lombardy Basin, Southern Alps). *Rivista Italiana di Paleontologia e Stratigrafia 127*, 3, 539–556.

Visentin, S., Faucher, G. & Erba, E. 2023: Calcareous Nannofossil Taxonomy and Biostratigraphy of the Toarcian-Lower Bajocian Colle di sogno section (Lombardy Basin, Southern Alps, Italy). *Rivista Italiana di Paleontologia e Stratigrafia 129*, 207–228. https://doi.org/10.54103/2039-4942/18615

Wiggan, N.J., Riding, J.B., Fensome, R.A. & Mattioli, E. 2018: The Bajocian (Middle Jurassic): a key interval in the early Mesozoic phytoplankton radiation. *Earth-Science Reviews 180*, 126–146. https://doi.org/10.1016/j.earscirev.2018.03.009